TECHNICAL REPORT STANDARD TITLE PAGE

1. Report No.	2. Government Accession No.	3. Recipient's Catalog No.
12.3		

4. Title and Subtitle	5. Report Date
Acoustic Radar and its Applicability to Highway Air Pollution Studies	June 1977
	6. Performing Organization Code

7. Author(s)	8. Performing Organization Report No.
August T. Rossano, Greg Bang, Paul C. Juhasz, Frank Carsey, and Franklin I. Badgley	

9. Performing Organization Name and Address	10. Work Unit No.
Water and Air Resources Division Dept. of Civil Engineering, FX-10 University of Washington Seattle, WA 98195	11. Contract or Grant No. Y-1540
	13. Type of Report and Period Covered
12. Sponsoring Agency Name and Address Washington State Highway Commission Highway Administration Building Olympia, WA 98504	Final Report
	14. Sponsoring Agency Code

15. Supplementary Notes
This study was conducted in cooperation with the U.S. Department of Transportation, Federal Highway Administration.

16. Abstract At the request of the Washington Department of Highways two studies have been conducted by a team of specialists at the University of Washington Air Resources Program to determine the applicability of the Acoustic Radar to air quality modeling of mobile sources. Following an exploratory investigation, a comprehensive study was undertaken in which the atmospheric structure was measured by a modified Monostatic Acoustic Radar and the derived stability conditions were compared with the commonly used Pasquill-Turner stability classes, which are based on empirical data. This comprehensive study was performed over a three month period in the fall of 1976, when an unusually persistent air stagnation existed in the study area caused by a stationary high pressure system over the entire Northwest. The Evergreen Point Floating Bridge Toll Plaza in Bellevue, Washington was selected for test location.

The carbon monoxide (CO) concentrations were measured at six strategically located sampling points and then compared with the computer model predictions utilizing atmospheric stability data derived by both the Pasquill-Turner and the Radar echo methods. The results indicated that the Acoustic Radar method of determining D & E stability classes is a more realistic approach than that of the Pasquill-Turner Method. Furthermore, the Radar method can also provide continuous remote sensing and recordings of atmospheric parameters.

The variation of the inversion height, as measured by the Radar echoes has shown a reasonably good correlation with the variation of the measured CO concentration.

17. Key Words	18. Distribution Statement
Acoustic Radar Air Quality Modelling Carbon Monoxide Predictions Transportation Pollution Remote Sensing Atmospheric Structure	

19. Security Classif. (of this report)	20. Security Classif. (of this page)	21. No. of Pages	22. Price
UNCLASSIFIED	UNCLASSIFIED		

Form DOT F 1700.7 (8-69)
HWY FORM 341-004 6/72

The Acoustic Radar and its Applicability to Air Pollution Studies

A Study
Prepared for the

WASHINGTON STATE HIGHWAY COMMISSION

DEPARTMENT OF HIGHWAYS

by

August T. Rossano
Greg Bang
Paul C. Juhasz
Frank Carsey
Franklin I. Badgley

University of Washington
College of Engineering
Department of Civil Engineering
Water and Air Resources Division
Seattle, Washington

December 1977

ABSTRACT

At the request of the Washington Department of Highways two studies have been conducted by a team of specialists at the University of Washington Air Resources Program to determine the applicability of the Acoustic Radar to air quality modeling of mobile sources. Following an exploratory investigation, a comprehensive study was undertaken in which the atmospheric structure was measured by a modified Monostatic Acoustic Radar and the derived stability conditions were compared with the commonly used Pasquill-Turner stability classes, which are based on empirical data. This comprehensive study was performed over a three month period in the fall of 1976, when an unusually persistent air stagnation existed in the study area caused by a stationary high pressure system over the entire Northwest. The Evergreen Point Floating Bridge Toll Plaza in Bellevue, Washington was selected for test location.

The carbon monoxide (CO) concentrations were measured at six strategically located sampling points and then compared with the computer model predictions utilizing atmospheric stability data derived by both the Pasquill-Turner and the Radar echo methods. The results indicated that the Acoustic Radar method of determining D & E stability classes is a more realistic approach than that of the Pasquill-Turner Method. Furthermore, the Radar method can also provide continuous remote sensing and recordings of atmospheric parameters.

The variation of the inversion height, as measured by the Radar echoes has shown a reasonably good correlation with the variation of the measured CO concentration.

Table of Contents

List of Tables

List of Figures

List of Photographs

The contents of this report reflect the view of the authors who are responsible for the facts and the accuracy of the data presented herein. The contents do not necessarily reflect the official views or policies of the Washington State Department of Highways or the Federal Highway Administration. This report does not constitute a standard, specification, or regulation.

1. Introduction

1.1 Background

Current techniques for Air Quality Modeling (1, 2, 3)* use the Pasquill-Turner stability classifications (4, 5) which are based on empirically obtained atmospheric data. An exploratory study of the University of Washington, of Acoustic Radar for characterizing atmospheric stability was sponsored by the Washington State Department of Highways in 1976. The executive summary of this study is included in Appendix A. Further studies by others have also demonstrated that the Acoustic Radar can be utilized for remote sensing of the atmospheric structure or (6, 7, 8, 9, 12).

At the request of the Washington State Department of Highways a comprehensive study was conducted by a team of specialists at the University of Washington Air Resources Program to determine the applicability of the Acoustic Radar to air quality modeling of mobile sources.

1.2 Purpose and Objectives

The purpose of this study is to determine whether or not the atmospheric stability information obtained by Acoustic Radar measurements provide viable alternatives to the empirically derived stability classifications of the Pasquill-Turner Method, and what additional information on air quality can be derived from acoustic radar data.

The main objectives of this study are as follows:

1. Compare air quality modeling results utilizing both stability derivation methods.

2. Correlate measured carbon monoxide concentration levels with atmospheric parameters derived by Acoustic Radar echoes.

3. Compare the conventional Pasquill-Turner stability derivation method with the method using Acoustic Radar Data.

* Numbers in parentheses refer to references on pages 68 and 69.

1.3 Outline of Study

In order to meet the stated objectives a number of tasks were determined as follows:

1. Install a monostatic Acoustic Radar unit and record the echoes during a predetermined test period.

2. Design and build a CO monitoring network and sample air at strategically selected points simultaneously with the radar measurements.

3. Set up a meteorological station and measure wind speed and direction during the test periods.

4. Determine atmospheric stability classes by the Pasquill-Turner Method (3), using meteorological data existing during the test period.

5. Determine atmospheric stability classes from the recorded Acoustic Radar echoes and compare them with the Pasquill-Turner stability classes established for the same time intervals.

6. Analyze the traffic pattern in the study area and obtain traffic parameters from existing State Highway Department records as well as by field measurements.

7. Calculate composite CO emission factors based on the traffic conditions existing in the study area during the test periods using the method developed by the Environmental Protection Agency (10).

8. Compute CO concentrations for the selected sampling points by means of the EPA-HIWAY Air Quality Diffusion Model (1) using the calculated emission factors and atmospheric stability parameters derived by the Pasquill-Turner method as well as from Acoustic Radar echoes.

9. Compare the computer results with the sampled CO concentration data.

1.4 The Study Area

The Toll Plaza of the Evergreen Point Bridge was selected for the study area. This bridge connects Seattle with Bellevue over Lake Washington as

shown in Figure 1 and has a highly congested traffic during the morning and evening rush hours. The vehicles from both directions have to stop at the toll booths and in rush hours long lines are formed by the queuing vehicles upstream of the toll booth in both directions. Since a toll is collected from all vehicles at the plaza, accurate records are available on traffic volume over the bridge. The main reasons for selecting this site for the study area were: the availability of traffic data, the high CO emissions from the queuing cars and the fact that there is no polluting industry located in the close neighborhood of the Toll Plaza which might effect the line source emissions.

A sketch in Figure 1 shows the location of the Evergreen Point Bridge and the study area. Figure 2 is a sketch of the Toll Plaza as a line source and Figure 3 depicts the locations of CO sampling sites in the study area. Photograph 1 is a view of the Toll Plaza looking east from the 76th Avenue N.E. overpass and Photograph 2 from the opposite direction looking west, toward Seattle.

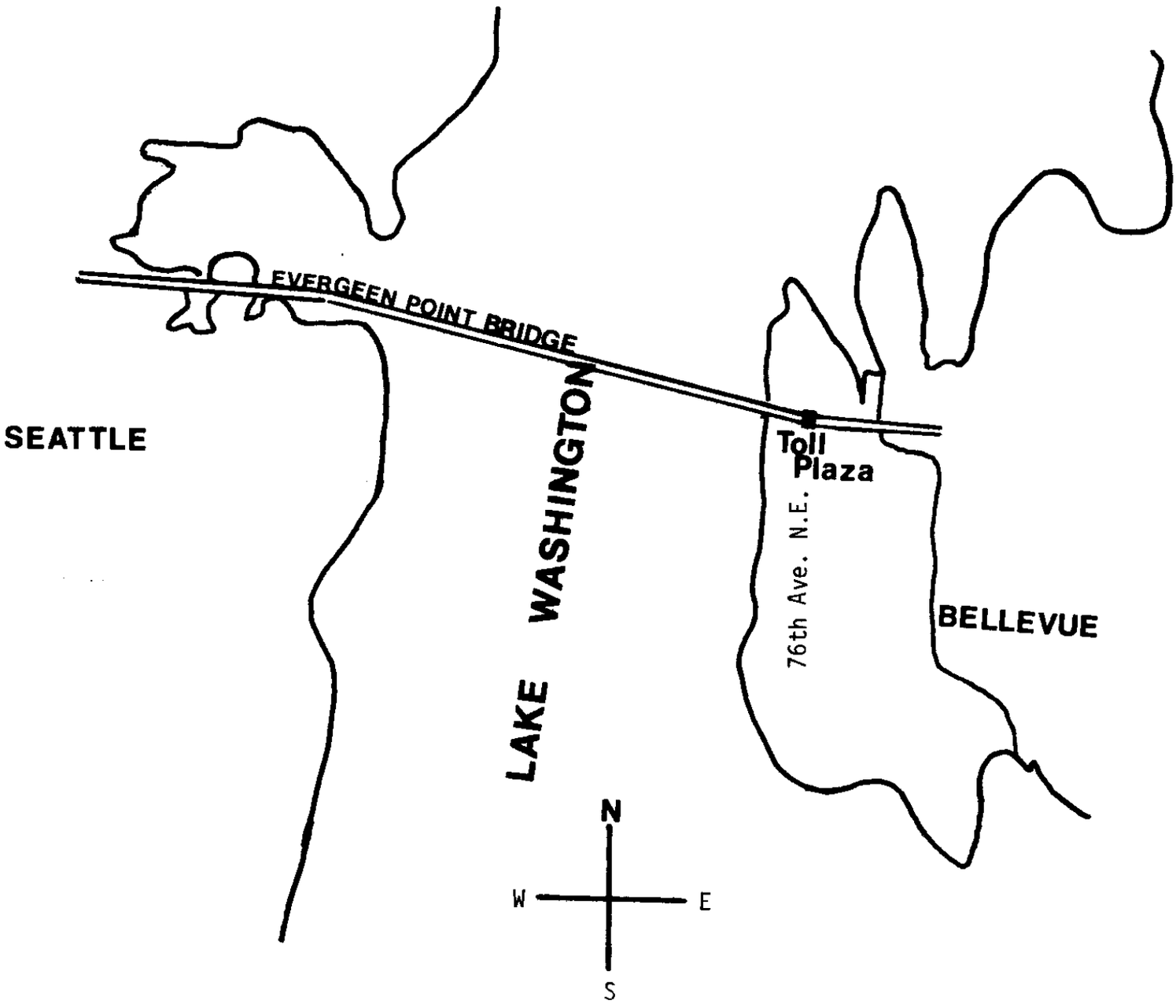

Figure 1. Location of Study Area

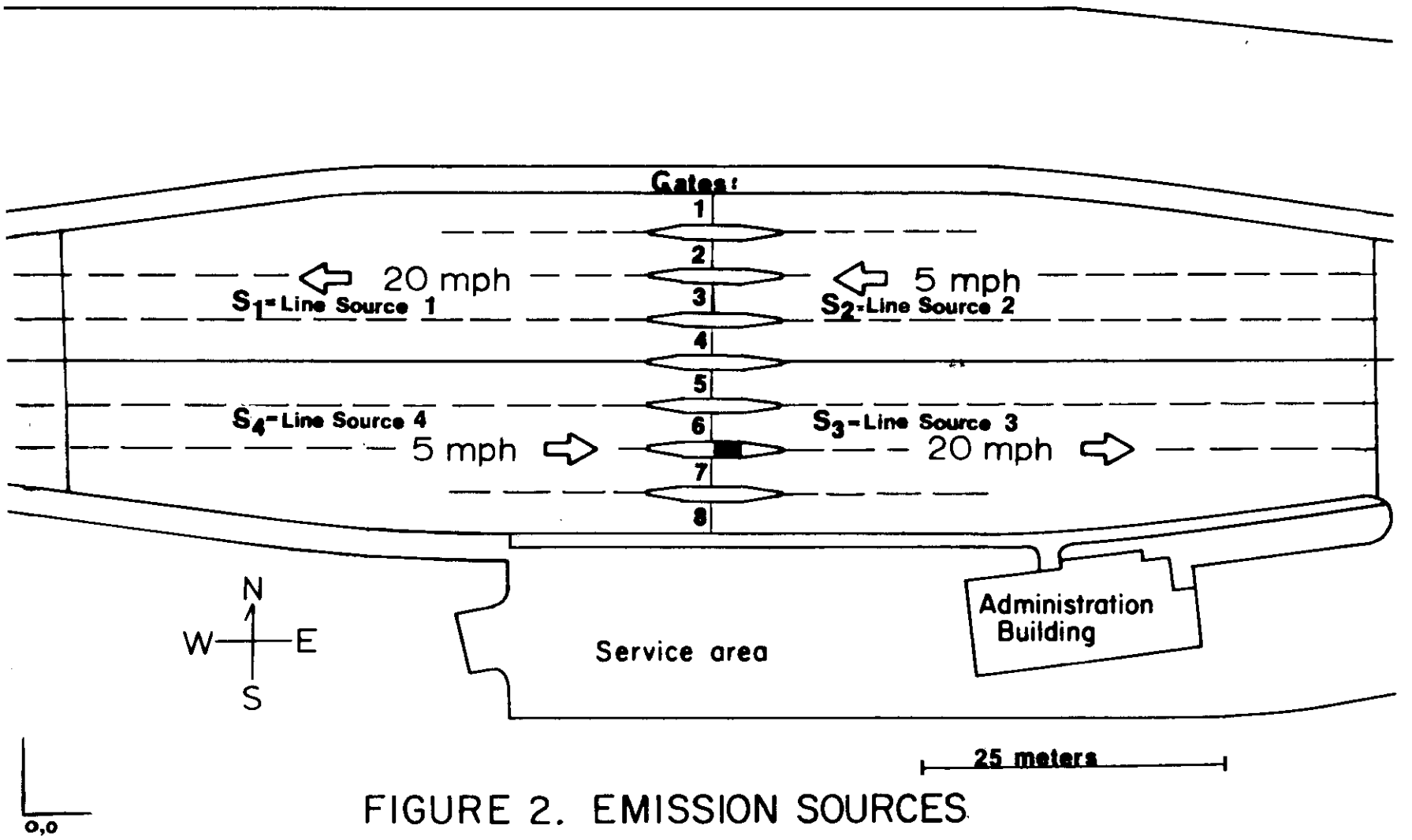

FIGURE 2. EMISSION SOURCES

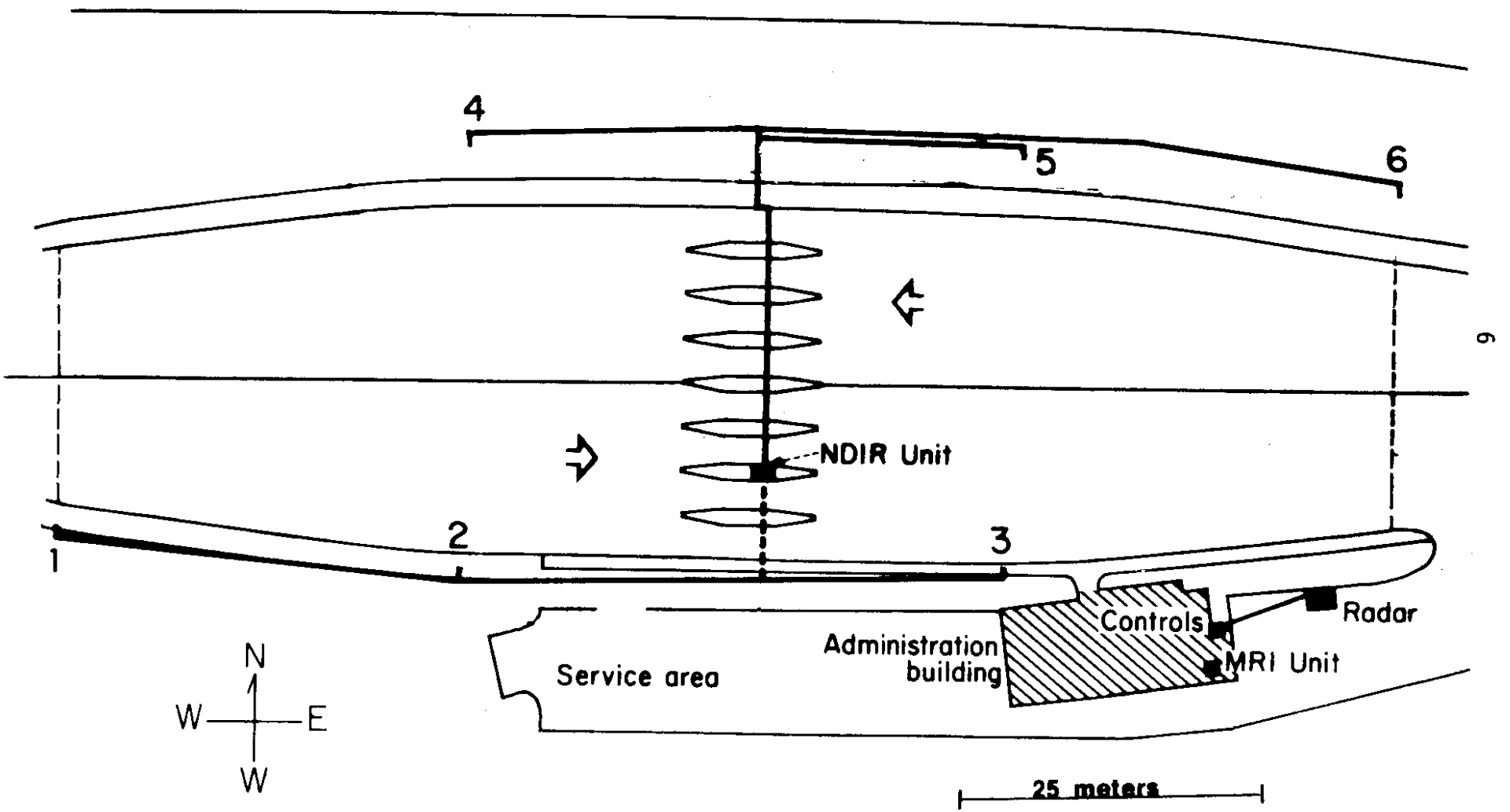

FIGURE 3. MONITORING NETWORK

Probes 1–6

Photograph 1. Toll Plaza Area –

Looking East from the 76th Avenue N.E. Overpass

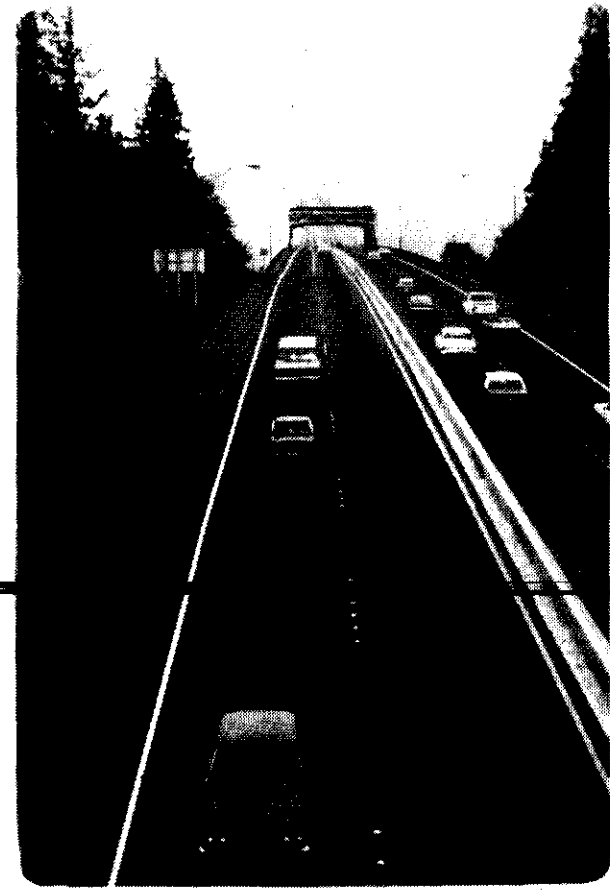

Photograph 2. West of Toll Plaza -

In the Background, the Evergreen Point Bridge

2. Data Collection Methods

The first step to reach the study objectives was to collect sufficient data in four major areas as follows:

1. Carbon monoxide emission from mobile sources. The emission factors were calculated using the EPA developed method (10). Inputs to this method were traffic parameters obtained from records and observations, and ambient temperature measured by the meteorological station.

2. Meteorological conditions were recorded by a meteorological station. Wind data were used to determine the Pasquill Stability Classes.

3. Carbon monoxide concentration. Ambient air was sampled at various points in the study area.

4. Acoustic Radar measurement of the atmospheric structure to determine air stability conditions.

Emission factors, meteorological data and stability classifications derived by either methods were used in air quality modeling to predict CO concentrations which then was compared with the existing conditions obtained by air sampling. The stability data were also utilized to compare the two methods of deriving stability classifications: either from empirical data as used in the Pasquill-Turner method or from radar echo records. A second utilization of the radar measurements was to correlate them with the CO concentration level in the study area. All data used for comparative purposes in the study were obtained simultaneously and at the same place. For practical purposes, continuous data recordings were made during most parts of the three month test period and only the rush hour data as worst existing conditions were utilized in the study.

Methods of collecting data in all four areas of interest, equipment used and data processing methods are discussed in the next chapters.

2.1 Emissions from Mobile Sources

The main reasons why the Evergreen Point Bridge Toll Plaza was selected for study area was the existence of heavy traffic conditions and the availability of traffic data. The traffic on the plaza is two-directional; there are peak periods associated with high vehicular density and slow movements; conditions which generate high carbon-monoxide emissions and well suited for stability and CO concentration studies. There is no polluting industry in the vicinity and the transportation here is responsible practically for the entire carbon monoxide emissions. The sampling results reflect the emissions from mobile sources in the area, and evaluation of traffice conditions supplies valid emission data. Tasks of carbon monoxide emissions evaluation included: traffic analysis, determination of traffic parameters, acquisition of traffic data and calculation of emission factors.

2.1.1 Traffic Description

The Evergreen Point Bridge connects Seattle across Lake Washington with Bellevue and Redmond. The purpose of trips are mainly commuting to and from work and characterized by two rush hour peaks, one in the morning from 0700 to 0900 hours and one in the afternoon between the hours 1600 and 1800. The traffic is moving in two directions with two lanes in both directions. There are eight toll booths in the Toll Plaza as shown in Figure 2; four are used for each traffic direction. All vehicles have to stop at the booth to pay the toll. In rush hours five booths are used in the congested direction and only three for the opposite traffic. The high traffic density at peak periods associated with stopping at the booth results in long lines of queuing vehicles backing up in each direction. In the morning the westbound traffic, moving toward Seattle is the heavy one, while in the afternoon the eastbound traffic is higher, but the westbound traffic is also considerable. Since there are only three gates open for the westbound traffic, the vehicle queuing is equally emphasized in both directions in the afternoon rush hours.

Both the morning and afternoon rush hours are considered worst emission cases and these hours were used to generate emission data for comparison purposes in this study. High traffic density, idling vehicles and stable meteorological conditions resulted in high CO concentrations during these periods.

2.1.2 Traffic Parameters

Traffic parameters affecting the rate of carbon monoxide emissions were the characteristics of vehicular movements in the area such as cruising speed, decelerating and accelerating rates, the duration of idling at the toll booths, the apparent speed of the tightly packed queuing cars advancing slowly toward the booths and the apparent speed of vehicles in a line source segment. An additional important parameter was the traffic density. Traffic parameters used for emission factor calculation are charted in Table 1.

2.1.3 Data Acquisition

Data on traffic volume were obtained from the Freeway Surveillance Group of the Washington State Highways Department District 1 office. These records gave information on traffic density in each direction accumulated in 15 minute intervals. Traffic volume information required for any vehicular movement analysis was obtained from immediate toll records and from field traffic counts.

The study area was divided into four line source segments (see Figure 2), the characteristics of vehicular movements were observed and analyzed, time measurements were made to determine the apparent speed in each segment at the worst case condition. A special emphasis was placed on the analysis of queuing characteristics since backed up traffic with idling vehicles are large contributors to the area CO emission (8). The traffic study is summarized in Appendix A. Based on this study, 5 mph was assumed as worst case apparent speed of vehicles approaching the toll booths and 20 mph for departing cars.

2.1.4 Emission Factors

Carbon monoxide emission factors were calculated using the method developed by the Environmental Protection Agency for (EPA) line sources. The method is described in Supplement 5 of Compilation of Emission Factors AP-42 (1). In this method composite emission factors are based on the mean emission factors established by the Federal Test Procedure (FTP) and then corrected for specific applications such as vehicle type, fraction of annual travel by year model, average speed, ambient temperature and starting conditions. These factors are defined as emissions in grams generated by one vehicle in one mile line segment and described by the equation:

$$E_{npstwx} = \sum_{i=n-12}^{n} \left(C_{ipn} M_{in} V_{ips} Z_{ipt} r_{iptwx} \right) \quad \text{(Equation 1)}$$

E_{npstwx} = is the composite emission factor in g/mi for calendar year n, pollutant p, average motor vehicle speed s, ambient temperature t, percentage cold start operation w, and percentage hot start operation x.

C_{ipn} is the 1975 Federal Test Procedure mean emission factor in g/mi for the i^{th} model year light duty vehicles for pollutant p during calendar year n.

M_{in} is the fraction of annual travel by the i^{th} model year light duty vehicles during calendar year n.

V_{ips} is the speed correction factor for the i^{th} model year light duty vehicle for pollutant p and average motor vehicle speed s.

Z_{ipt} is the temperature correction factor for the i^{th} model year light duty vehicles for pollutant p and ambient temperature t.

r_{iptwx} is the hot/cold vehicle operation correction factor for the i^{th} model year light duty vehicles for pollutant p, ambient temperature t, percentage cold start operation w, and percentage hot start operation x.

2.1.5 Emission Prediction

Evaluation of CO emission in the study area was made in several steps as follows:

1. The area was divided into four source segments, as shown in Figure 2. These sources can be described with reference to the toll booth as follows:

Source 1. Eastbound approach lanes

Source 2. Eastbound departure lanes

Source 3. Westbound approach lanes

Source 4. Westbound departure lanes

The length of source segments 1 and 4 is 186 feet while segments 3 and 4 are 200 feet long. These lengths were determined by the utility poles where the measurements were made. The number of lanes in each source segment depended on the number of booths used in the direction of traffic.

2. The traffic density of rush hour periods was established for each directional traffic. Both hourly and 15 minute average traffic density were used in the study.

3. Typical emission factors were calculated for each source segment (gram/mile/vehicle) and multiplied with the traffic density (vehicle/hour) to predict source emission in gram/mile/hour which was converted to the input form required by the used air quality model (gr/m/sec).

2.1.6 PSAPCA Program for Emission Estimation

Emissions were calculated by the use of a computer program developed by the Puget Sound Air Pollution Control Agency (PSAPCA) which used data specifically compiled for use in the State of Washington. The required inputs to the program and the rationale behind their selection are charted in Table 1. The emission computer model is programmed for percent of travel by model-year typical for King county. Emission factors can be corrected for speeds starting with 5 mph in 5 mph steps. The traffic study (Appendix B)

Table 1. Input Values to PSAPCA Emission Program

Year:	1977	Data obtained Oct.-Dec. 1976 but a large percentage of 1977 model vehicles were already in use.
County:	King	The study area is in King County.
% Hot Start:	0%	Assumed all vehicle trips originated outside of 500 seconds (a) driving time (Seattle or Bellevue).
% Cold Start:	0%	
Vehicles/Period:	variable	Determined by official traffic count, obtained from the Department of Highways.
Number of Lanes:	3 or 5	Dependent on the number of toll booths used in the direction of traffic and time of day the emission is calculated.
Ambient Temperature:	45°F	Average measured by the meteorological station.
% Heavy Duty Gas Vehicles:	2%	Used by PSAPCA for King County traffic.
Speed:	5, 20 mph	Speeds determined by actual averaged measurements for rush-hour periods. (See Appendix B)

Notes: (a) Cold start is defined (10) as over four hour engine-off period and less than 500 seconds operation, after start. The effect of 10% cold start is evaluated in Table 8.

resulted in apparent speeds of 3.9 mph and 21 mph for approaching (queuing) and departing traffic respectively, but the nearest rounded figures of 5 mph and 20 mph were used for inputs.

Emission factors were calculated for 0% cold start condition. This assumption was based on the fact that during the morning rush-hour, vehicles were backed up in excess of a quarter mile. At the queuing speed (Appendix A) three to five minute traveling time was required to reach the Toll Plaza area. Over 500 seconds motor run is considered hot run steady state operation (1). There are very few residents within a three to five minute drive to the line-up on the freeway. Therefore, by the time any vehicle reached the impact area (Toll Plaza), the engines have been running at least eight minutes which indicates that most vehicles were in a stabilized phase. However, since the exact traveling time of the vehicles from start-up to impact area was unknown, a transient cold start phase between 0 to 10% may be expected. The effect of higher percent of cold start is evaluated in Table 8.

2.2 Meteorological Conditions

2.2.1 Recording Station

A meteorological station was erected on top of the Administration Building to measure wind speed and direction. The equipment used was an MRI battery-operated unit which can measure the ambient temperature, the wind direction, and the wind speed. These data were recorded mechanically onto a self-contained, pressure-sensitive strip chart. The location of the meteorological station is shown in Photograph 3.

2.2.2 Meteorological Data

Wind direction and wind speed data were used to determine the Pasquill-Turner atmospheric stability classifications (4, 5). The percentage of

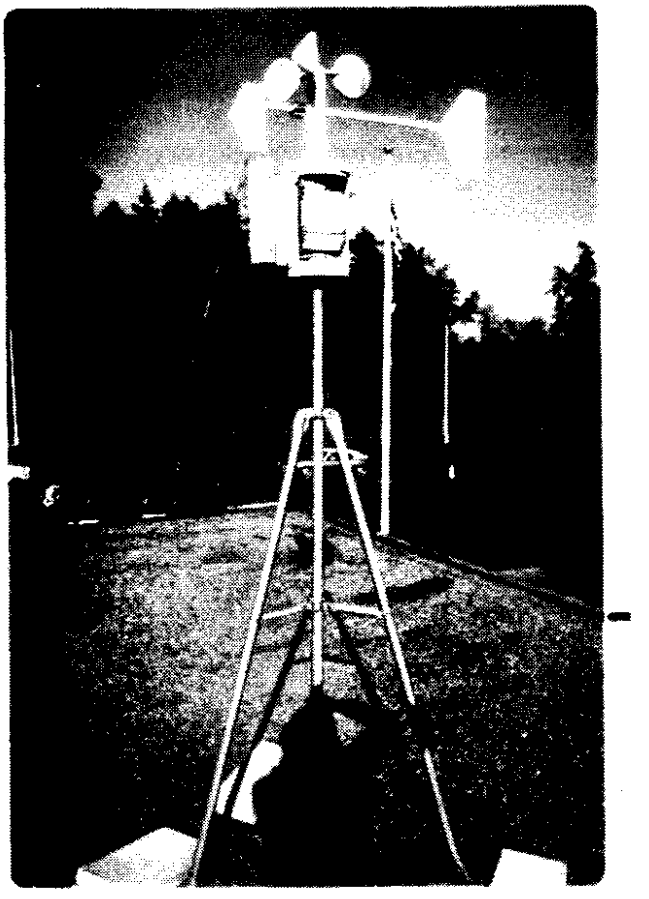

Photograph 3. Meteorological Station

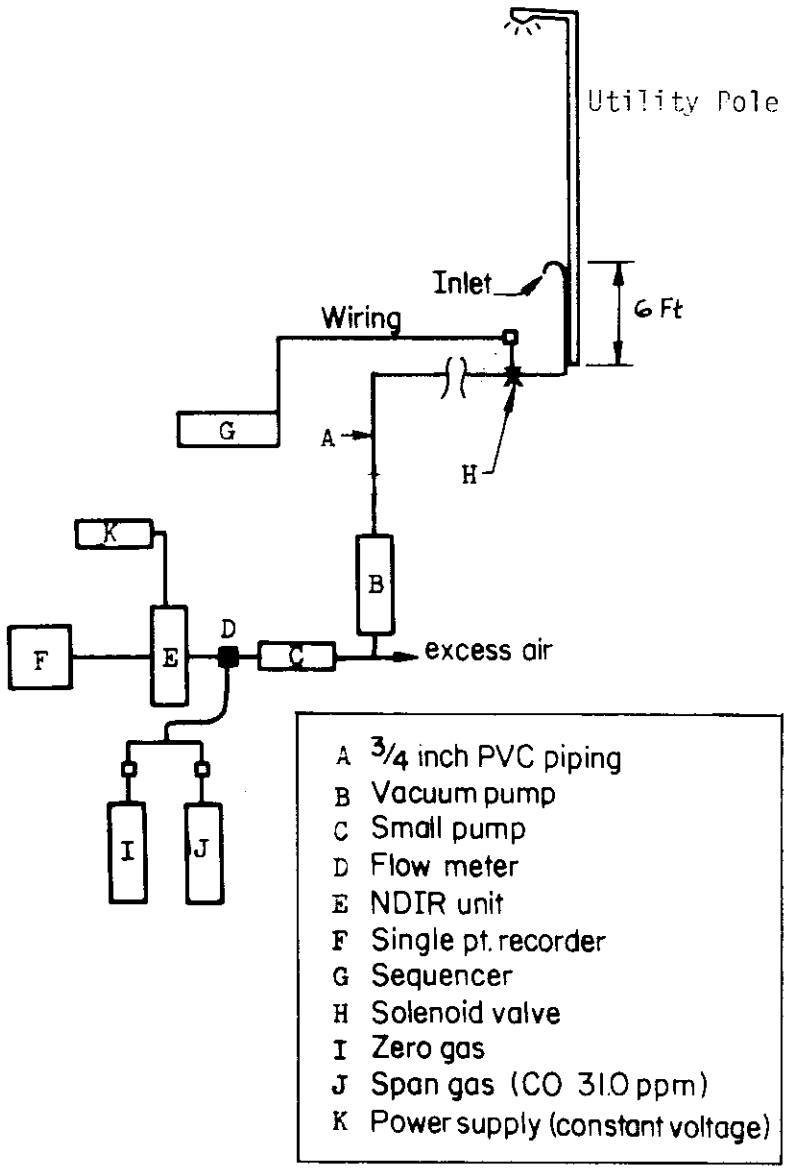

Figure 4. Sampling Network Schematic

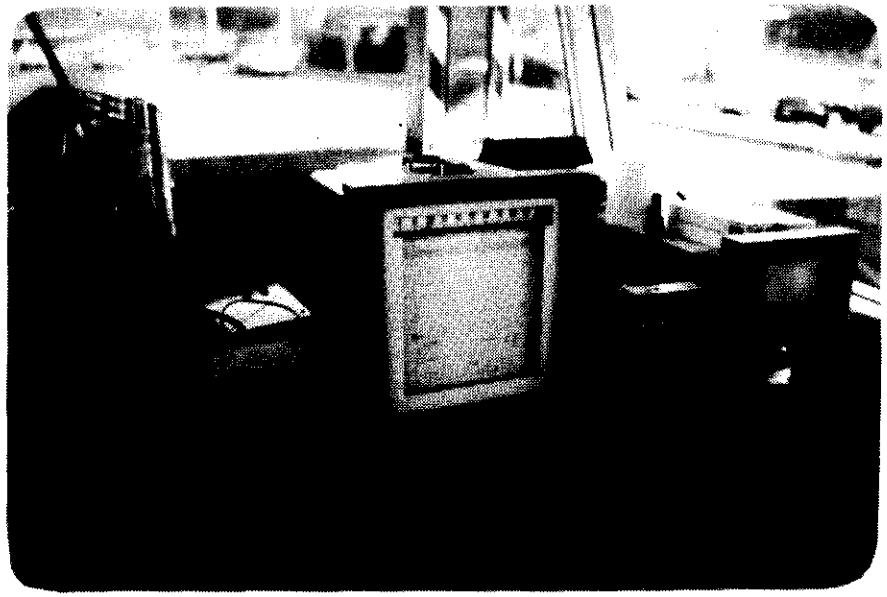

Photograph 4. Monitoring Equipment in Toll Booth #2

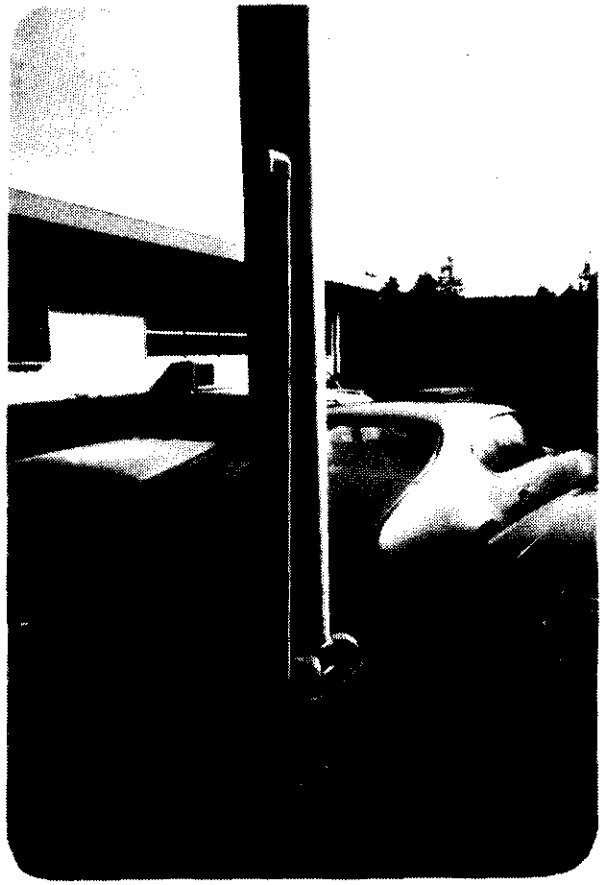

Photograph 5. Location of Sampling Probe #3 on a Utility Pole

tained from District 1 Office, Department of Highways. Power to the Infrared Analyzer was supplied by a constant voltage source (K).

2.3.2 Infrared CO Analyzer

The CO levels were measured by a Beckman Infrared Analyzer, Model 315B, which automatically and continuously monitors CO concentration (14). The Beckman non-dispersing type Infrared Analyzer (NDIR) measures the differential absorption of infrared energy through a sample gas energy beam and a reference gas energy beam. The instrument uses a double beam optical system. The sample cell incorporates a flow-through tube carrying a continuous stream of sample gas. The reference cell is a sealed tube filled with a reference gas. The beams of radiation are blocked simultaneously 9.25 times per second by a chopper. The presence of the infrared-absorbing component of interest (CO) in the sample stream causes a difference in energy levels between the two cells in the system. The differential energy increment is then converted to an electrical signal which was calibrated to indicate CO concentration in ppm. A functional diagram of the Infrared Analyzer is shown in Figure 5. Specifications for the Model 315B are listed in Appendix C.

2.3.3 Sampling Data

Air was sampled at six points as shown in Figure 3 using one probe at a time for one minute period in numerical sequence of the probes. The total cycle time of the sampling was six minutes. Continuous monitoring of the air quality provided information on CO concentration levels recorded graphically as ppm vs elapsed time. The area under each cycle was averaged by visual approximation and the resulting six minute concentration levels were further averaged to determine the hourly CO concentration levels for each investigated peak traffic periods.

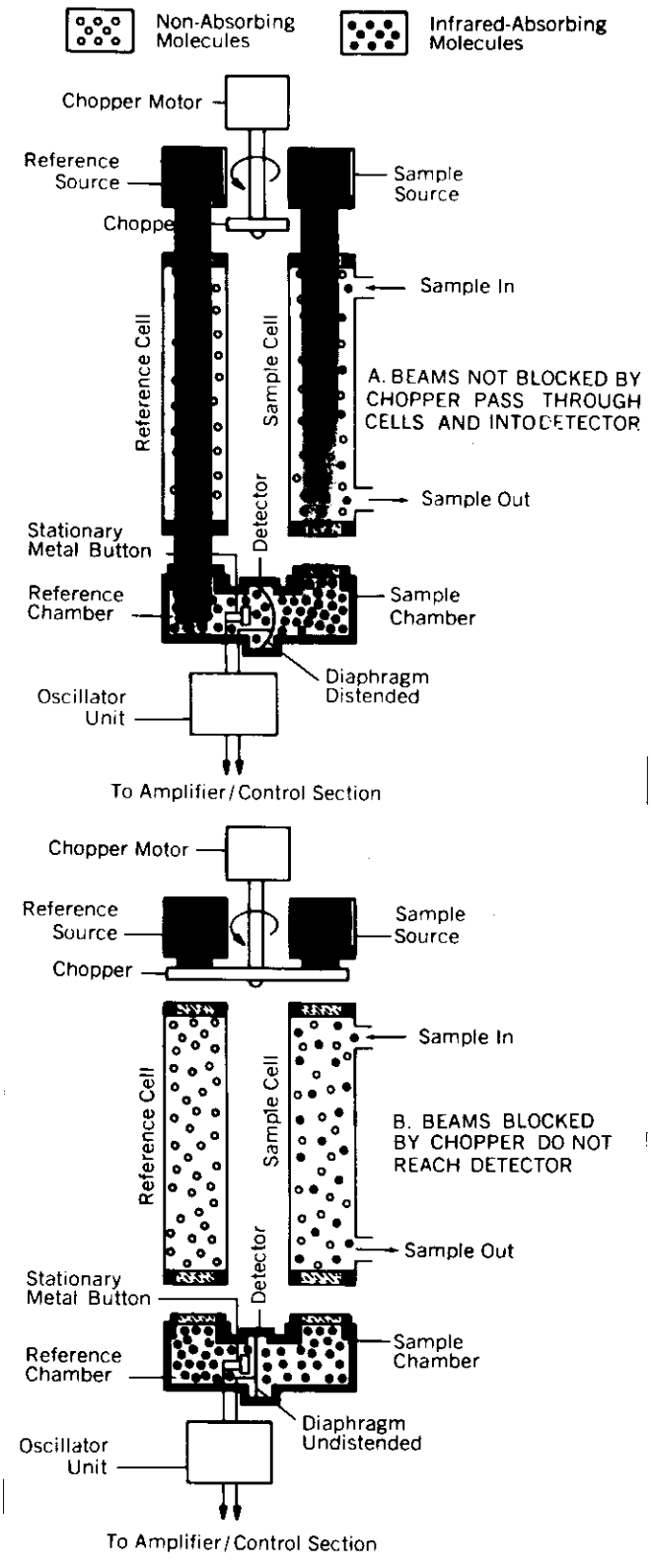

Figure 5. Functional Diagram of the Infrared Analyzer

2.4 Acoustic Radar Measurements

2.4.1 Fundamentals

Acoustic energy (sound) propagates through the atmosphere as a longitudinal wave of pressure variations. The velocity of sound propagation is proprotional to the square root of the atmospheric temperature ($C^2=C_o^2(1 + T/To)$, where C and Co are velocities of sound in disturbed and undisturbed atmosphere respectively, measured in m/sec, T is the temperature of the disturbed atmosphere and To is the mean atmospheric ambient abosolute temperature).

Acoustic waves are scattered by temperature and velocity inhomogeneities in the atmosphere. The time delay between a transmitted sound signal and its received echo, assuming the local speed of sound is known, will provide information on the altitude the echo was scattered back.

An instrument which generates and transmits acoustic pulse, receives and processes the backscattered energy (echo) returned by the atmosphere is called an Acoustic Sounder. Because of the analogy between its operation with acoustic waves and the operation of Radar (Radiation Detection and Ranging) with electromagnetic waves, other descriptive terms for an Acoustic Sounder are: Acoustic Radar and Sodar (Sound Detection and Ranging). If the returning scattered signals are collected by the same antenna which transmits the signal the system is called monostatic. In a bistatic system antennas, different from the receiver and some distance removed, are used for signal generation. Monostatic radar measures only the thermal structures of the atmosphere, while a bistatic system also measures wind structure based on the principle of Doppler frequency shift.

In this study a monostatic system was used and the word Acoustic Radar refers to a monostatic Acoustic Sounder equipment.

Scatterers in the atmosphere which provide the echoes for a monostatic system are temperature inhomogeneities (actually speed of sound inhomogene-

ities). The sound travels 331.5 m/sec in dry air at 0°C and the speed increases at 0.6 m/sec for each °C above 0°C. The Acoustic Radar used in this study generated 2700 Hz signal, and the vertical scale was calibrated for a sound speed of 333.3 m/sec which corresponds to an air temperature of 3°C. In order to generate an echo, the inhomogeneities should have at a scale of one half of the wavelength of the transmitted signal. For a 2700 Hz signal this scale is about

$$\frac{333.3 \text{ m/sec}}{2700 \text{ cycle/sec}} \frac{1}{2} = .08 \text{ m/cycle} = 8 \text{ cm/cycle}$$

A turbulent field has turbulences at all wavelengths thus there will always be some scattering back of the acoustic signal. Temperature variation required is only a small fraction of a degree.

The acoustic waves are attenuated as they propagate through the atmosphere and with the distance. Furthermore, scattering can occur in any direction. Thus a selected single echo received by the radar has only a small fraction of the energy of the transmitted signal. The Radar instruments have to provide for amplification of this weak echo as well as for filtering out undesirable environmental noises.

2.4.2 Monostatic Acoustic Radar

The Acoustic Radar system used in the study is a modified Monostatic Acoustic Radar, Model 300, manufactured by Aerovironment, Inc., Pasadena, California. Data from the Acoustic Radar is recorded and used to determine inversion and mixing characteristics of the initial 300 meters of the atmosphere, with the capability of measuring greater heights. The Model 300 emits a brief 2700 Hz(2700 cycles per second) pulse and receives the echo backscattered from turbulence aloft(see Figure 6). The stylus on the recorder moves across the paper so the position on the chart represents height(Z_i) in the atmosphere.

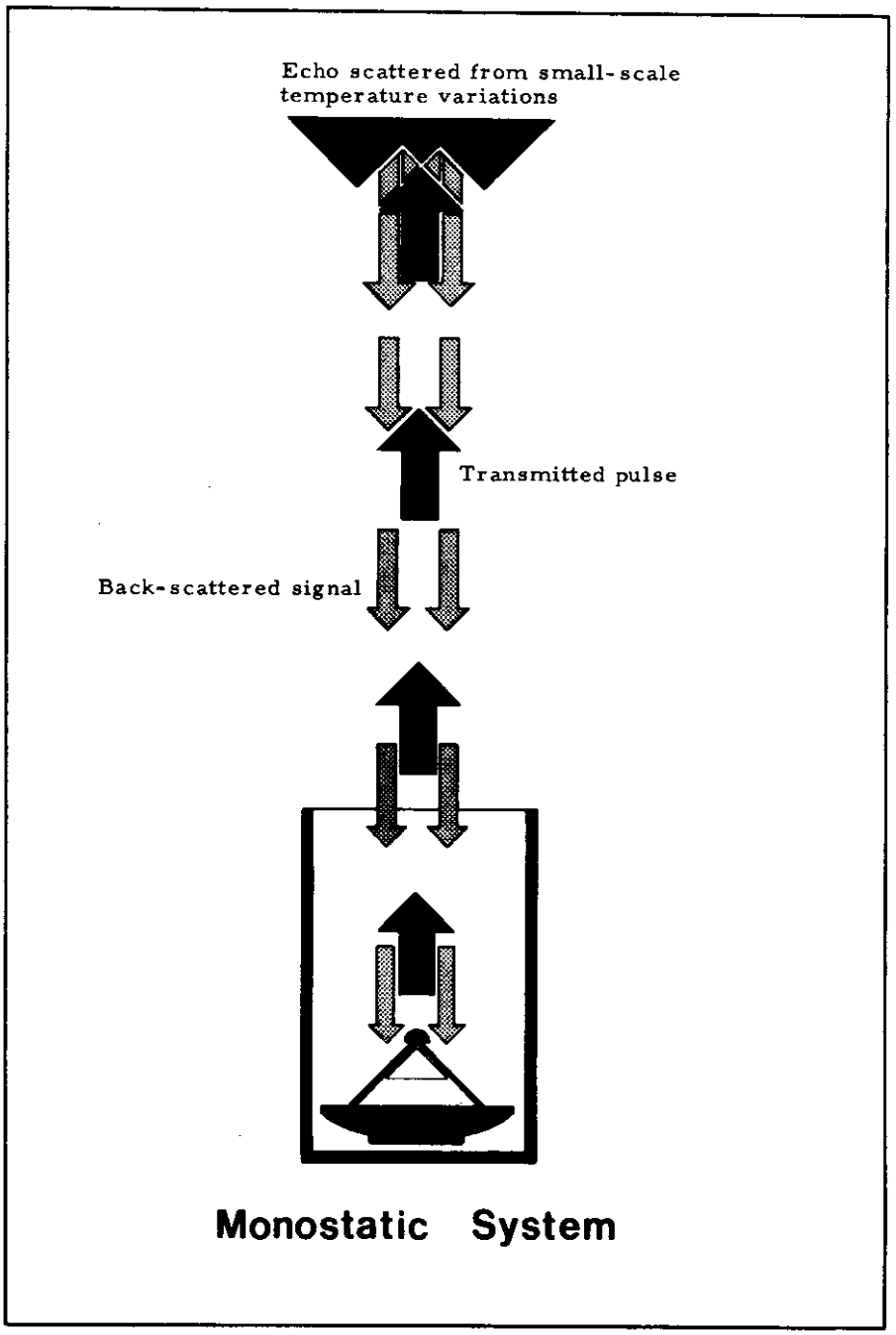

Figure 6. Monostatic Acoustic Radar Operation Schematic(14)

The stylus darkens the specially treated paper by electrical erosion. The degree of darkness is proportional to the strength of the backscattered signal received by the antenna.

The receiving antenna was designed and built at the University of Washington (See Appendices A and D). It was specifically designed for use in close proximity to highway traffic, to cut down as much background noise as possible.

Photographs 6 through 9 show the disassembling of the radar antenna and its method of transportation. It takes at least two persons four hours to either assemble or disassemble the unit.

2.4.3 Atmospheric Data Recorded by Acoustic Radar

The only meteorological feature which gives an echo on a Monostatic Acoustic Radar is one which causes temperature microstructure field, that is turbulence which is mixing across a "non-neutral" temperature gradient (see Chapter 3.1 for discussion of neutral or adiabatic gradient). Turbulences which can produce echoes are as follows:

1. The temperature gradient is unstable and the air mixing is dominated by thermally driven convective motions. Echoes produced by these atmospheric conditions are called "thermal echoes" and give vertical spikes on the radar chart. Thermal echoes are indicators of unstable atmospheric conditions.

2. The temperature gradient is stable and air mixing is caused by wind shear. The echoes resulting from these mechanical turbulences are called "shear echoes". These predominantly horizontal echo regions mark the turbulent interface between two layers of air. Shear echoes provide information on the height of mixing layer and temperature inversion, which is associated with stable atmospheric conditions. Stability conditions and interpretation of echo records are discussed in more details in chapters 3.1 and 3.3 respectively.

Photograph 6

Acoustic Radar Antenna - Disassembling Starts

Photograph 7

Acoustic Radar Antenna - Sound Absorbing Shield Removed

Photograph 8

Acoustic Radar Antenna. Radar Unit Exposed.

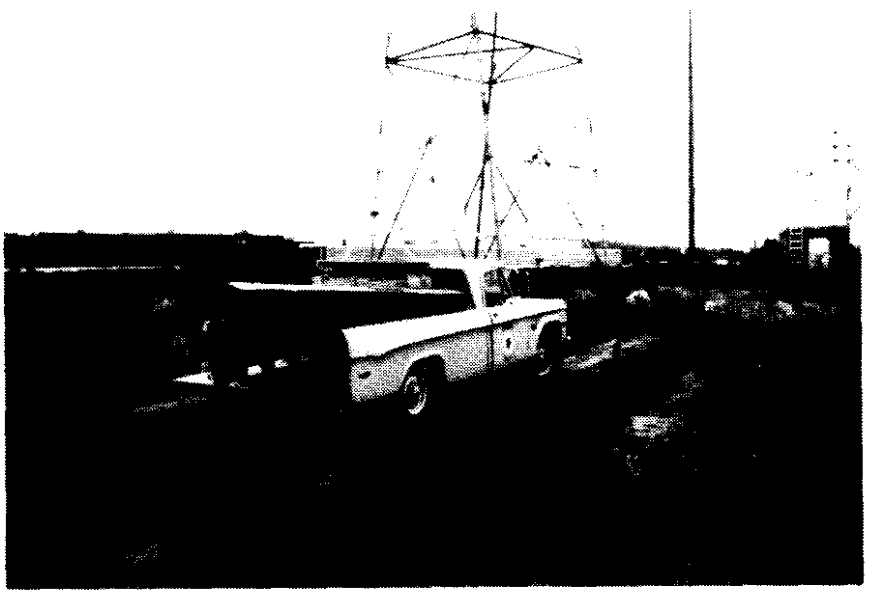

Photograph 9

Transportation of Disassembled Acoustic Radar Antenna

recorded the echoes on a facsimile chart. The characteristics of recorded echoes were then analyzed to generate information on atmospheric stability conditions for air quality modeling. The charted echo data were also utilized in the CO concentration correlation study.

3. Atmospheric Stability

A key factor affecting the dispersion of air pollution is the depth of the layer of the atmosphere within which pollutants emitted near the surface are mixed. The extent of vertical mixing is regulated by the stability of the atmosphere. A stable or stagnating region puts limits on the vertical dispersion. Determination of atmospheric stability is a primary requirement in predicting air quality by dispersion models.

3.1 Interpretation of Stability (15)

The rate of change of the atmospheric temperature with the height is called the lapse rate. If the air temperature decreases with the height, the warmer air on the ground or in lower layers moves up. This vertical air motion introduces also turbulences and the atmosphere becomes unstable. On the other hand, in case of "inversion", when the temperature of air rises with an increase of altitude, the result is suppressed vertical air motion and the atmospheric condition became stable. Thus the temperature changes of the atmosphere or lapse rate is a good indicator of atmospheric stability. The basis used to compare the various lapse rates and the resulting stability of the air is the dry adiabatic lapse rate, when the temperature of dry air decreases with altitude and the temperature gradient is 5.4 °F for every 1000 feet. In this case the air is "neutrally" buoyant. If the temperature decreases faster than this rate, the air is said to be unstable. The greater the temperature gradient, the greater the mixing of the lower layer. In the same respect, if the temperature changes at a lower or inverse rate, the air is said to be stable, with less mixing. Vertical air motion is enhanced if the atmosphere is unstable and suppressed if the atmosphere is stable. Figures 7 and 8 illustrate lapse rates and interpretation of air stability.

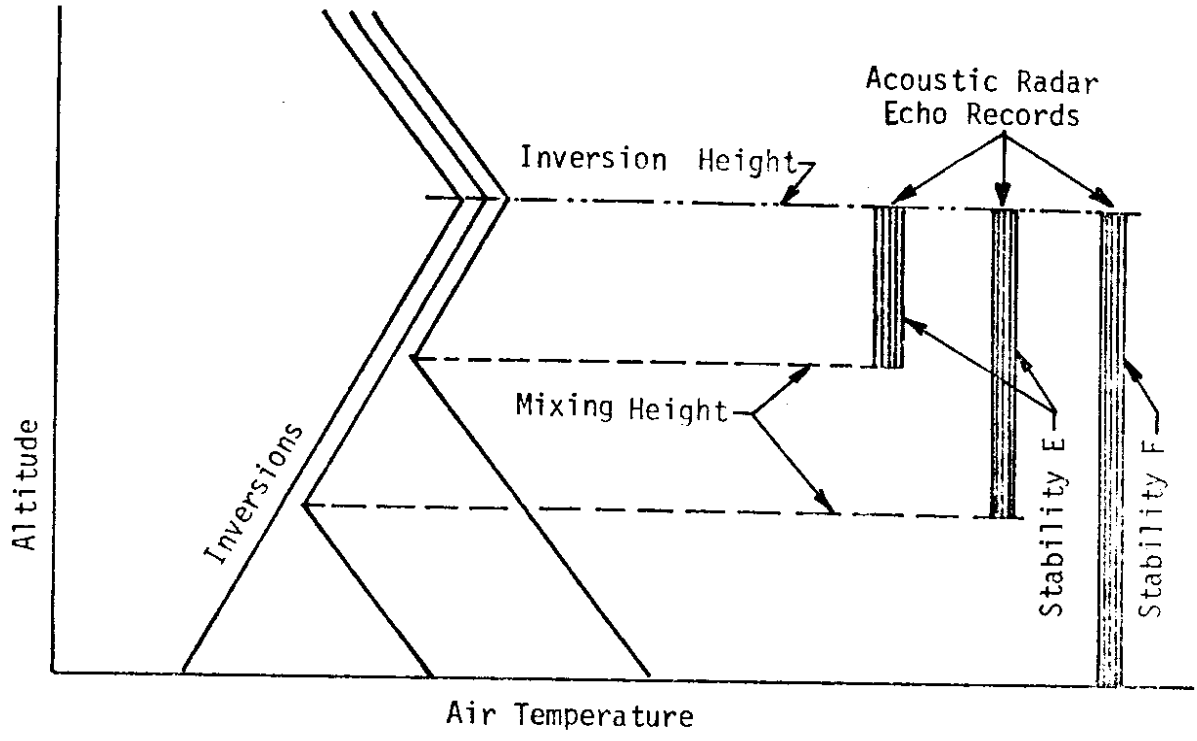

Figure 7. Definition of Mixing Height and Inversion Height (7)

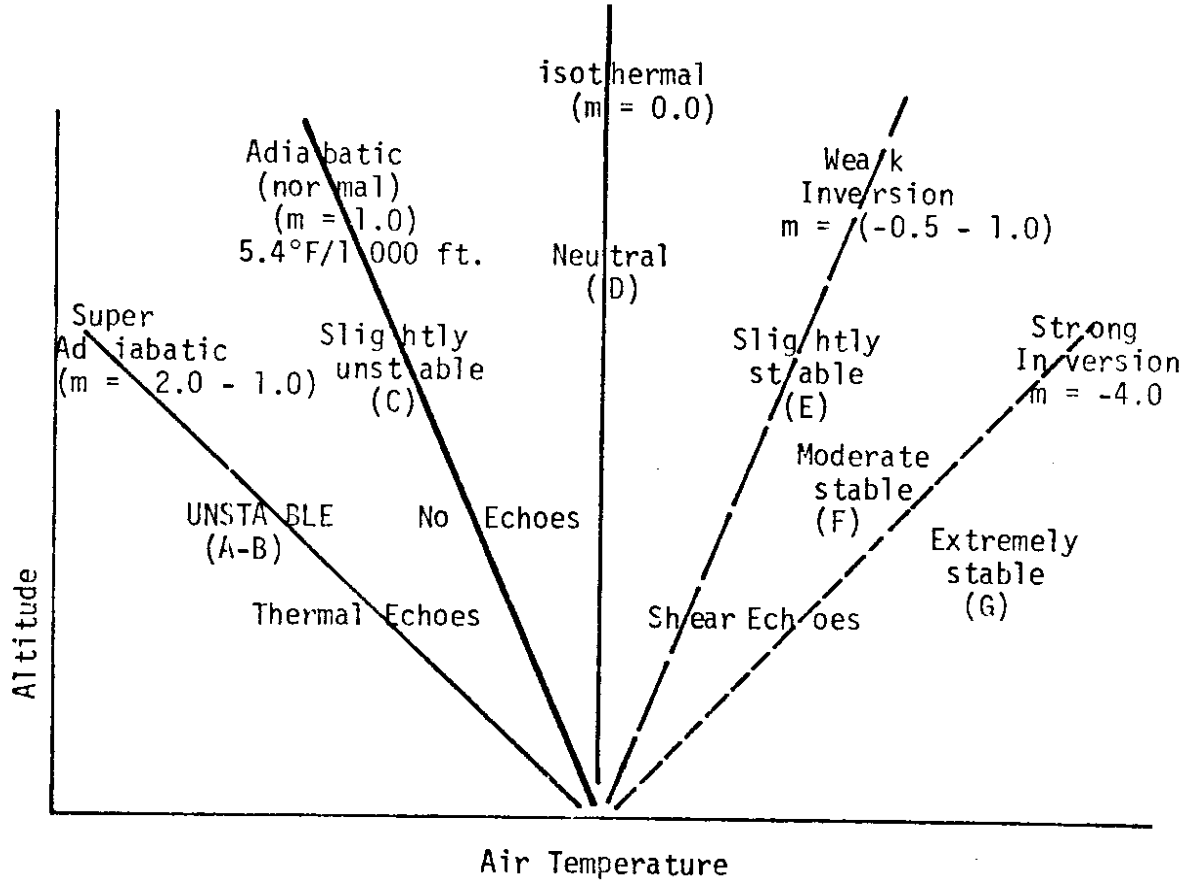

Figure 8. Air Temperature vs Height (17)

The temperature gradient and consequently the degree of stability is primarily dependent upon the solar radiation and wind conditions which are influenced by the percent of cloud cover and the solar incident angle.

Atmospheric parameters such as wind speed, temperature change, cloud cover, etc. are utilized in predicting atmospheric stability. At stable atmospheric conditions the emitted pollutants are trapped under the stable layer and result in high concentration levels. On the other side unstable conditions are associated with good mixing and low pollutant concentration.

3.2 Pasquill-Turner Stability Classification

The stability of the lower atmosphere can give a good indication of pollutant mixing and dispersion. In 1961 F. Pasquill classified the air stability into six groups based on observations of seasonal and annual wind distribution. D.B. Turner interpreted these stability classifications as dependent on various atmospheric parameters such as cloud cover, solar incident angle and wind speed. This Pasquill-Turner stability classification method first appeared in the Journal of Applied Meteorology in February, 1964 (4) and is outlined in Appendix E.

Pasquill-Turner Stability categories (5) are charted in Table 2. Class A is the most unstable and class F is the most stable condition. Night period refers to a period from one hour before sunset to one hour after sunrise.

The Pasquill-Turner Stability classifications are based on empirical data. For air quality modeling wind speed was measured and averaged over an investigated period. The cloud cover was estimated by visual observation.

3.3 Stability Determination Using Acoustic Radar Echoes

As discussed in chapter 2.4 the monostatic Acoustic Radar records the echoes scattered back by turbulent fluctuation of temperature of the atmosphere. Two distinct types of radar echoes are as follows:

Table 2. KEY TO STABILITY CATEGORIES (5)

Surface Wind Speed (at 10 m), m sec^{-1}	Day			Night	
	Incoming Solar Radiation			Thinly Overcast or ≥4/8 Low Cloud	≤3/8 Cloud
	Strong	Moderate	Slight		
< 2	A	A-B	B		
2-3	A-B	B	C	E	F
3-5	B	B-C	C	D	E
5-6	C	C-D	D	D	D
> 6	C	D	D	D	D

The neutral class, D, should be assumed for overcast conditions during day or night.

"Strong" incoming solar radiation corresponds to a solar altitude greater than 60° with clear skies; "slight" insolation corresponds to a solar altitude from 15° to 35° with clear skies.

1. Thermal echoes are generated by vertical mixing where the temperature gradient is unstable and mixing is dominated by thermal driven convective motions. Thermal echoes are represented by vertical lines on the facsimile chart as shown in Figure 9.

Thermal echoes are indicators of strong convection and unstable atmospheric conditions which are categorized as stability classes A and B by the Pasquill-Turner Method.

2. Shear echoes or shear turbulence echoes are echoes scattered back from regions where there is a turbulence powered primarily by wind shear and characterized by disorganized motion. The shear echo is most common in a region with a stable temperature profile but strong wind turbulence, although it can also occur in unstable situations, say next to the ground, when the mixing is dominated by turbulence rather than by organized convection. The shear echo with a stable temperature situation above the ground typically marks the division between two distinct air masses. For practical purposes the shear echo traces on the recorder represent the depth of mixing layers of

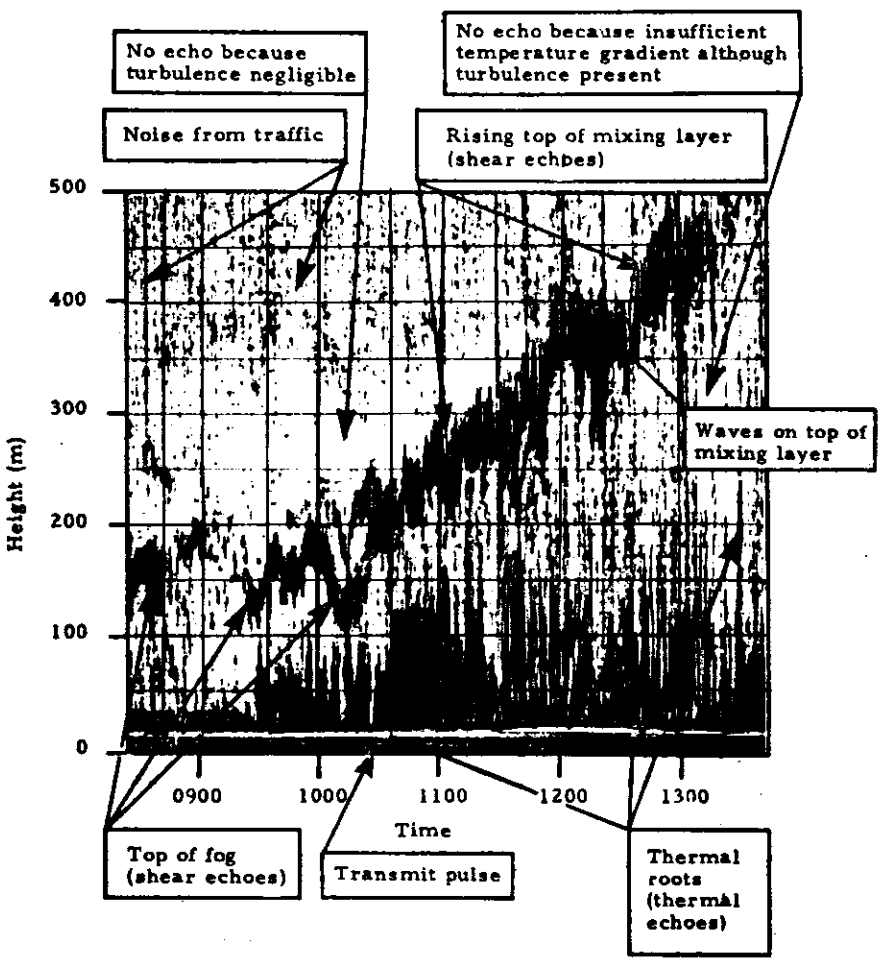

Figure 9. Monostatic Acoustic Radar Records (16)

the atmosphere. I. Tombach and M. Chan conducted research on estimation of mixing depth and inversion height by Acoustic Radar (7). In their study the mixing height in the acoustic sounding records was defined as extending up to the base of the acoustic echo and the inversion height was defined by the top of the acoustic echo as shown in Figure 7. In this study (7) close correlation was found between radar echoes, mixing heights and inversion heights, measured by radio sound and aircraft soundings.

Stability classification derived from Acoustic Radar data has been reported by Carsey et al. by analyzing the data based on 1 hour averages (Appendix A).

By comparing the various stability determinations, it was found that the Acoustic Radar derived mixing layer height was at least a reasonable indication.

Shear echoes are indicators of temperature inversion and stable atmospheric conditions. Low level inversion (represented by the top of the shear echo trace on the facsimile chart) with mixing layer (the base of the shear echo trace) above ground, identifies stability class E, while low level inversion reaching the ground represents stability class F in the Pasquill stability category.

No echo phenomena indicate either no turbulence or the temperature profile condition is neutral so that there are no local temperature variations due to turbulence. In either case there is no temperature microstructure to give echoes. In these cases, or when the inversion layer is high, the stability conditions are relatively neutral as categorized by the Pasquill-Turner stability classes between C and D.

The Acoustic Radar stability classifications and the corresponding Pasquill-Turner stability classes are charted in Table 3.

Table 3. Acoustic Radar Stability Classification (6)

Stability Class	Criteria	Echo Type
A & B	Strong convection; needle-like acoustic radar traces from the plumes	thermal
C & D	Lack of trace or high inversion	none
E	Low level inversion with mixing below	shear
F & G	Low level inversion reaching the ground	shear

4. Dispersion Modeling

4.1 Gaussian Plume Dispersion Model

There are many mathematical dispersion models available, which attempt to simulate the action of the atmosphere in mixing and transporting pollution from its source to some receptor location downwind. The EPA-HIWAY Air Pollution model chosen for analysis in this study is based on the Gaussian Plume Model, which assumes that the concentrations of pollutants within the plume generated by the vehicles on the highway are distributed normally, with respect to the Gaussian model, in both the crosswind and vertical directions (5). The equation for the solution of the concentration at a receptor downwind from a point source is given by Turner (5).

$$C_{(x,y,z,H)} = \frac{Q}{2\pi\sigma_y \sigma_z u} \exp\left[-\frac{1}{2}\left(\frac{y}{\sigma_y}\right)^2\right] \left\{\exp\left[-\frac{1}{2}\left(\frac{z-H}{\sigma_z}\right)^2\right] + \exp\left[-\frac{1}{2}\left(\frac{z+H}{\sigma_z}\right)^2\right]\right\} \qquad \text{(Equation 2)}$$

where:

C = concentration at point x,y,z, (g/m^3)

x = horizontal distance downwind in the direction of mean wind, (m)

y = crosswind distance, (m)

z = height above ground level, (m)

Q = emission rate term, (g/sec)

σ_y, σ_z = standard deviation of plume concentration in horizontal direction and vertical directions.

u = mean wind speed, (m/sec)

H = effective height of emission source, (m)

4.2 Description of EPA-HIWAY Air Pollution Model

The EPA-HIWAY model is a Gaussian Plume Model which estimates pollution concentrations for an "at grade" highway, where highway emissions are

considered to be equivalent to a series of finite line sources (1). Each lane of traffic is modeled as though it were a straight finite line source. The highway is placed in a grid system to locate endpoints of the highway segments and receptor locations. Each lane is placed in the grid by the program at locations corresponding to the lane width and median width. The wind direction is specified by the user in degrees from north (North = 360° ∿ 0°) (1). Determination of the pollutant concentration downwind of the highway entails simple trapezoidal integration of a series of point sources located along this line source. The model assumes that the concentration varies linearly between two calculated points, so that the integrated value between the two points is the average of the concentrations normalized for source strength from the two points, multiplied by both the distance between the points and the line source emission rate (1).

4.3 Computer Model Input

In this study four line segments were defined according to EPA-HIWAY model specifications. Each segment is depicted in Figure 2 by one of the four coordinates of the sectioned highway. Emission rates for each segment were calculated and entered into an Input Format for EPA-HIWAY. An Input Format which describes the variables entered into the model is shown in Table 4, while Table 5 is a listing of the actual data input into the model for November 3, 1976.

4.4 Carbon Monoxide Concentration Prediction

The contribution of each line source is displayed in parts per million (ppm) of CO for each of the six receptors. The data were then tabulated to examine the total contribution of CO to each receptor from the four line sources. Table 6 is a summary of the data output for November 3, 1976.

Table 4. EPA HIWAY Input (Definitions)

DATE:	Date measurement occurred
TIME PERIOD: (hours)	Time measurement made
LINE SOURCE:	Defined in Figure 2 (a)
LINE END POINTS: (x,y, meters)	Specified in a coordinate system (b)
EMISSION HEIGHT: (z, meters)	0.0 (emission source on ground)
WIND DIRECTION: (0 to 360°)	Averaged over a one hour period. When wind was variable multiple wind directions were analyzed (c)
WIND SPEED: (m/sec)	Averaged over a one hour period
INVERSION HEIGHT: (meters)	Averaged over a one hour period derived by Acoustic Radar
STABILITY:	Averaged over a one hour period derived by either Pasquill-Turner or Acoustic Radar Methods
# LANES:	3 to 5 lanes for each line source depending on the traffic conditions (d)
SOURCE STRENGTHS: (gr/m-sec-lane)	Number of vehicles times the emission factor (e)
ROAD WIDTH: (meters)	14.6
MEDIAN WIDTH: (meter)	0.0
# RECEPTORS:	6
RECEPTOR LOCATIONS: (x,y,z) (meters)	Specified in a coordinate system (b)

NOTES:
(a) Four line sources in the study area
(b) x=0 at sampling probe #1 location, y=0 at 19.5 m south of the road edge.
(c) North is 360° or 0°
(d) Normal traffic conditions 4 lanes in each direction. During peak periods 5 lanes used in the direction of high traffic and 3 in the low traffic movement.
(e) Calculated by PSAPCA computer program using traffic parameters determined for the time period above and converted to gm/m sec

Table 5. EPA HIWAY Input (Sample)

DATE:	November 3, 1976
TIME PERIOD:	0700 - 0800
LINE SOURCE:	S_1
LINE END POINTS: (x,y, meters)	(0, 29.3) (56.7, 29.3) (a)
EMISSION HEIGHT: (z, meters)	0.0
WIND DIRECTION:	225°
WIND SPEED (m/sec)	1.0
INVERSION HEIGHT: (meters)	100.0
STABILITY:	5 (E) (b)
# LANES:	3
SOURCE STRENGTHS: (gr/m-sec-lane)	.013316 (c)
ROAD WIDTH: (meters)	14.6
# RECEPTORS: (x,y,z, meters)	6 (d)
RECEPTOR LOCATIONS: (x,y,z, meters)	R1 = (0, 23.2, 1.8) R2 = (31.7, 19.5, 1.8) (a,d,e) R3 = (75.6, 19.5, 1.8) R4 = (31.7, 61.0, 1.8) R5 = (76.8, 53.7, 1.8) R6 = (108.5, 51.2, 1.8)

NOTES:
(a) x=0.0 at sampling probe #1 location, y=0.0 at 19.5 m south of the road edge.
(b) Numerical sequence is assigned to stability classes (A=1, E=5)
(c) Composite emission factor calculated = 2.466×10^{-5} gm/m-sec-lane. (The total traffic density in 3 lanes is 1620 vehicle/hour eastbound (3 gates are open eastbound). Total emission rate of source #1 = $(2.466 \times 10^{-5})(1620)/3 = 0.013316$ gm/m-sec-lane.
(d) The sampling probe locations were selected for receptor sites for concentration prediction.
(e) z = height of probe location = 1.8 m

Table 6. Predicted CO Concentration (ppm) for Receptors

Wind direction = 210°
Stability = E

Line Source (see Figure 2)	Receptor (see Figure 3) 1	2	3	4	5	6
1	.691	.186	.00	6.716	1.516	.000
2	.00	.00	.00	1.472	.043	.000
3	.000	.00	.00	11.533	20.723	20.065
4	.00	.00	.052	.306	1.853	2.777
Total	.691	.186	.052	20.027	24.135	22.842

In most cases wind direction was difficult to interpret because of light and variable winds. However, by inspection of both wind sensor strip chart and CO chart records an approximate wind direction was determined.

4.5 Comparison of Sampled and Computer Predicted CO Concentrations

The measured values of CO were averaged for the downwind sampling probes which, in this case, were probes 4, 5, and 6. The measured CO concentration was 18 ppm for the time period 0700 to 0800 on November 3, 1976 (see Figure 11). Atmospheric stability class during this period derived by both methods was F. The measured CO concentrations were compared to the predicted concentrations which averaged 22 ppm for the three receptors at locations 4, 5 and 6. With an assumed background concentration of 2 ppm (13, 18), this will equal to 24 ppm. In this case the computer model overpredicts the actual measured value by 6 ppm.

Concentrations at wind directions of 180° and 225° were also analyzed in the same manner as in the previous example and the results were listed in Table 7. Results of two other tests were also tabulated in this table.

Table 7. Comparison of Measured and Computer Model Predicted Average CO Concentration Levels (a)

Date	Stability	Measured CO	Model Predicted CO Concentration(d)			
			Wind Direction	Stability Class		
				D	E	F
10.29.76	E(b,c)	20.7	180°	19.0	18.6	
			210°	22.1	23.0	
			225°	25.4	26.8	
11.3.77	F(b,c)	17.7	180°	17.1	18.2	18.6
			210°	21.5	22.3	23.0
			225°	24.5	25.9	27.1
11.23.77	D(b), E(c)	9.8	180°	15.0	15.5	
			210°	18.1	18.8	
			225°	20.5	21.6	

Notes: (a) For all downwind receptors 4, 5, and 6, at morning rush hours. All concentration levels in ppm. Measured and predicted values are averaged for 1 hour periods.
(b) Stability derived by Pasquill-Turner Method
(c) Stability derived by Acoustic Radar Method
(d) Add 2 ppm background concentration for predicted values

Table 8. The Effect of the Percent of Engine Cold Start on CO Concentration (a)

Date	Stability	Measured CO ppm	Model Predicted CO		
			Wind Direction	Cold Start 0%	Cold Start 10%
10.29.76	E	20.7	210°	19.0	27.0
			225°	25.4	37.9

Notes: (a) Measured and predicted values (ppm) averaged for 1 hour period
(b) Actual stability derived by both: Pasquill-Turner and Acoustic Radar Methods

The stabilities for each day were determined by the Pasquill-Turner method and the Acoustic Radar method. The stability derived by the two methods were the same for the 10.29 and 11.3 tests. On 11.23 the stability determined by the Pasquill-Turner method was D, while the Acoustic Radar method measured E class.

Table 8 shows the computed concentration levels utilizing 10% cold start as compared to 0% cold start used in this study and calculated in Table 7 for the day of October 29, 1977.

In all cases the computer model predicted CO concentrations, calculated for the test periods (Tables 7 and 9) were higher than the sampled results. One cause of this high computer prediction may be the uncertainty in determining accurate wind data in case of low wind speeds and variable winds, which is an important variable in the EPA-HIWAY model.

5. Results

5.1 Comparison of CO Concentration and Acoustic Radar Data

In order to establish relationship between Acoustic Radar measurements of inversion heights and CO concentration levels the quality of air in the study area was continuously monitored for several two-hour periods between September and December. During the same periods the atmospheric structure above the study area was also measured in continuous manner by the Acoustic Radar. The date and time of these period, which were selected for analysis in this report, are charted in Table 9.

Table 9. CO and Radar Data Acquisition Periods

Date		Figure Number
10/29/76	0700 to 0900	10
11/03/76	0700 to 0900	11
11/03/76	1600 to 1800	12
11/23/76	0730 to 0930	13

Three of these periods were morning rush hours, one was the afternoon peak traffic period. The traffic volume was also recorded during these periods. The results were plotted in Figures 10 through 13 as a function of elapsed time as follows:

1. The upper curve is the traffic count (N_v), the number of vehicles eastbound and westbound. Traffic data are the number of vehicles passed the toll booth in 15 minute intervals and were taken from the toll booth listings.

2. Carbon monoxide (CO) concentration levels in parts per million(ppm) were plotted in the center. Air was sampled in 6-minute intervals at 6 probes in sequential order starting with probe #1 for one minute. After sampling at probe #6 the sampling network switched back to probe #1 to start a new cycle. The CO data in above Figures are 6-minute averages of CO sampled at three probes on the downwind side of the highway (see Figure 3).

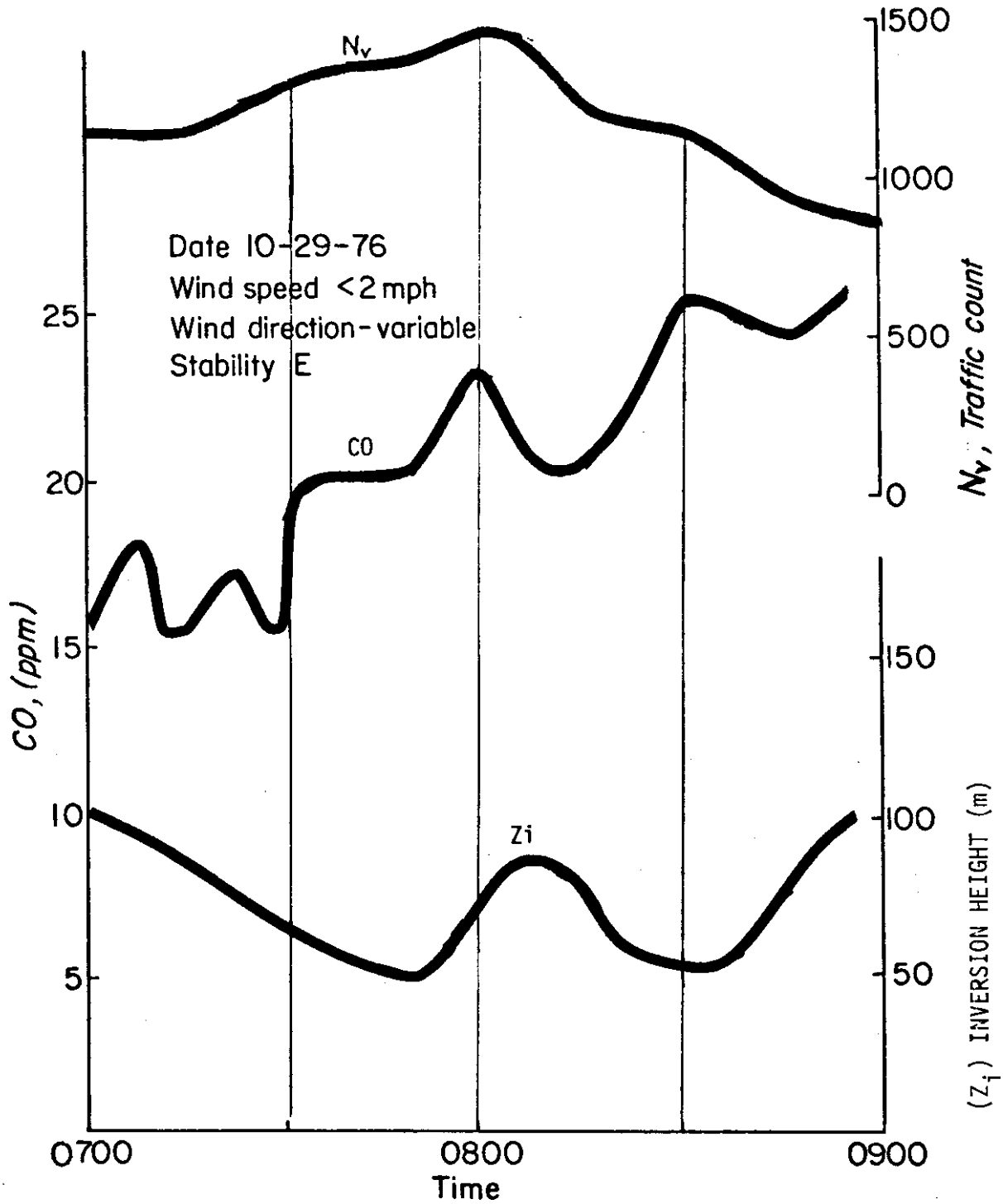

Figure 10. Comparison of Acoustic Radar Data

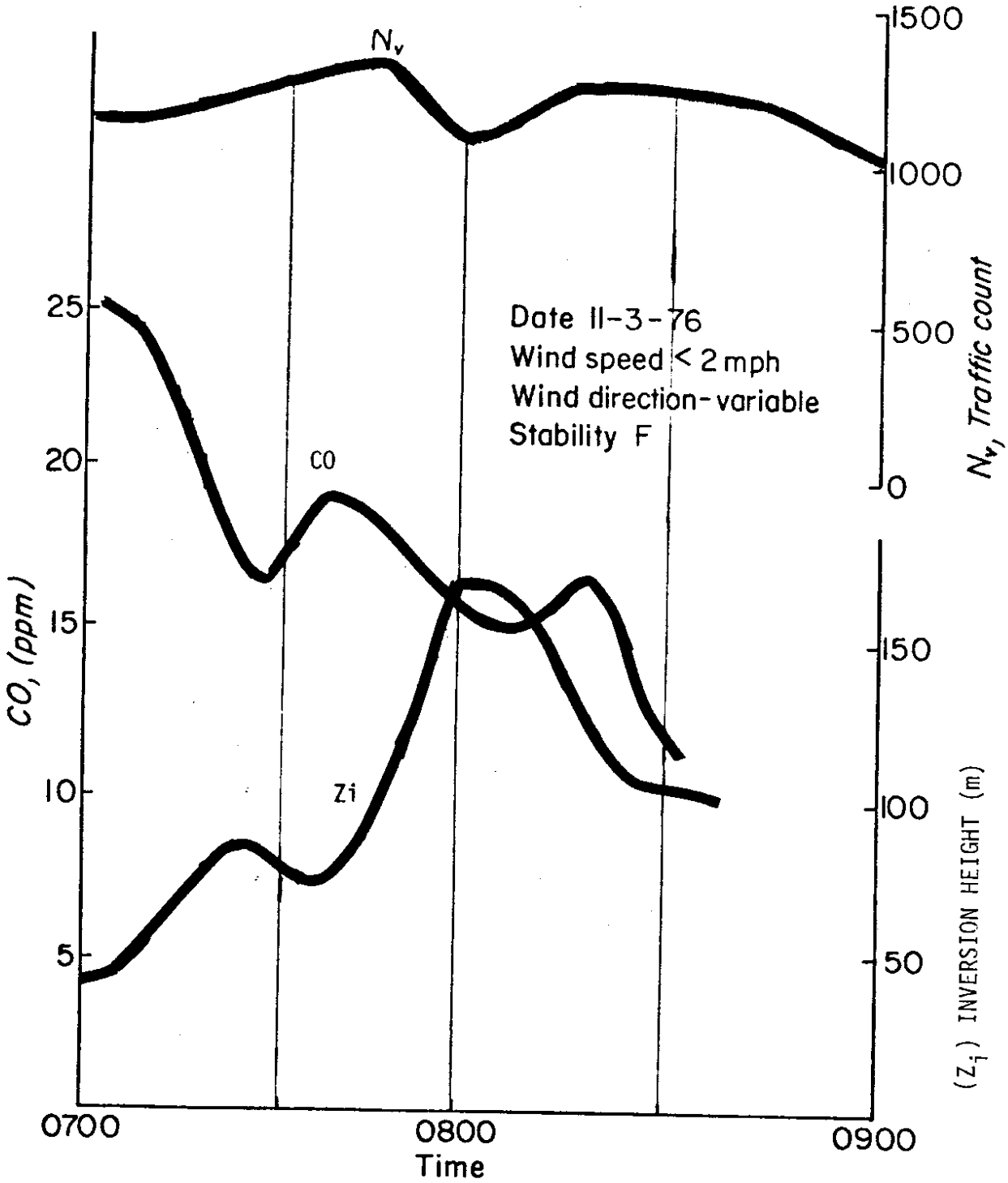

Figure 11. Comparison of Acoustic Radar Data

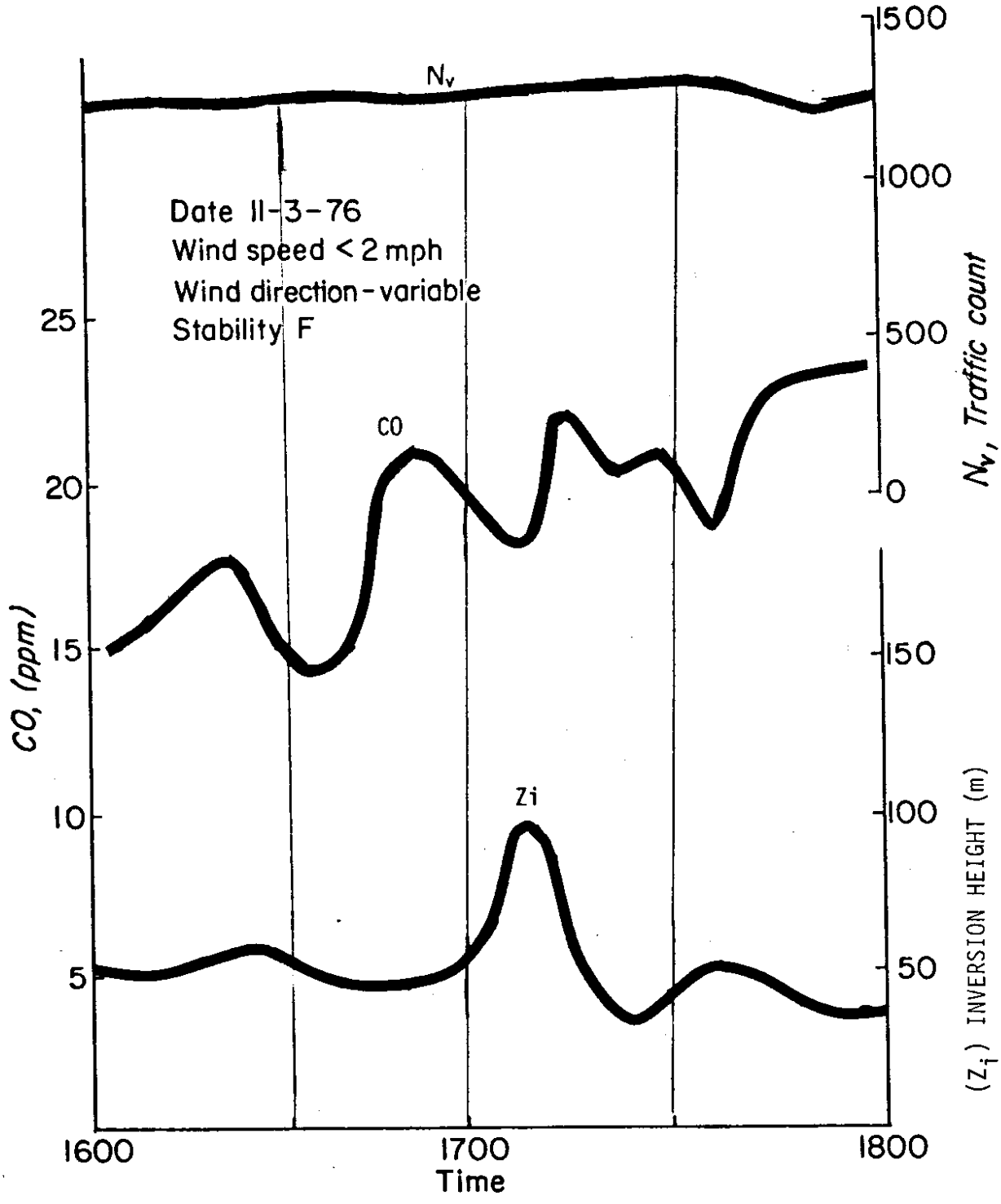

Figure 12. Comparison of Acoustic Radar Data

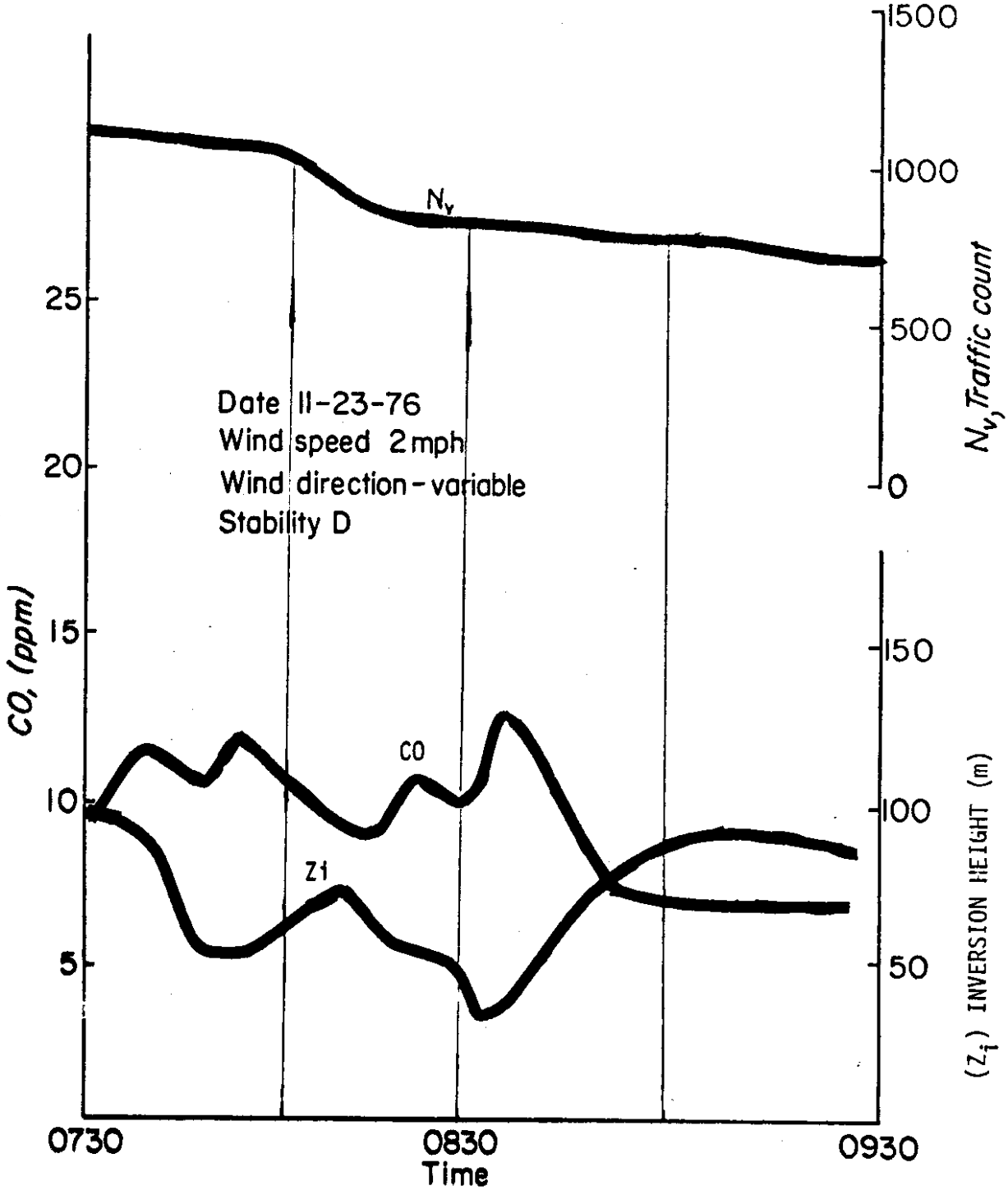

Figure 13. Comparison of Acoustic Radar Data

3. The lower curve shows the variation of temperature inversion heights (Z_i) of the atmosphere in meters above ground level measured by the Acoustic Radar (see Chapter 3.3). This curve connects the top points of the recorded shear echoes. Wind speed, wind direction, and atmospheric stability data are also shown in each figure, averaged over the two hour period.

5.2 Acoustic Radar Records

Typical radar records are shown in Figures 14 through 17. These pictures are high contrast photographs of the Acoustic Radar data overlayed with corresponding CO concentrations, on lower register, and traffic count on upper register. Looking at the Radar records, the dark band across the bottom represents the transmitted signal, the narrow clear space is a delay before the echo is received, and the darker areas above represent echo returns. The vertical lines running from the top to the bottom of the trace come from external noise, such as traffic and aircraft.

Figure 14 is a record taken on Saturday, November 20, 1976 showing convective air movement between 1300 and 1400. Then rather abruptly they are replaced by a stable surface layer resulting from a possible change in the cloud cover fraction. The thermal echoes are distinguishable by their rather dark and spear-like appearance. Multiple, discontinuous layers are present on the last half of the radar record starting about 1600. Note that there is a maximum in CO concentration and minimum mixing height at 1600, and a minimum CO concentration and maximum mixing height at 1700. Figures 15 through 17 are representative weekday mornings, associated with characteristic rush-hour maximum CO concentration and minimum inversion height between 0730 and 0830. There is a maximum inversion height and minimum CO concentration between 1200 and 1300 for each of the days cited. The days were mostly overcast, with partial afternoon clearing and light winds of 2-3 mph.

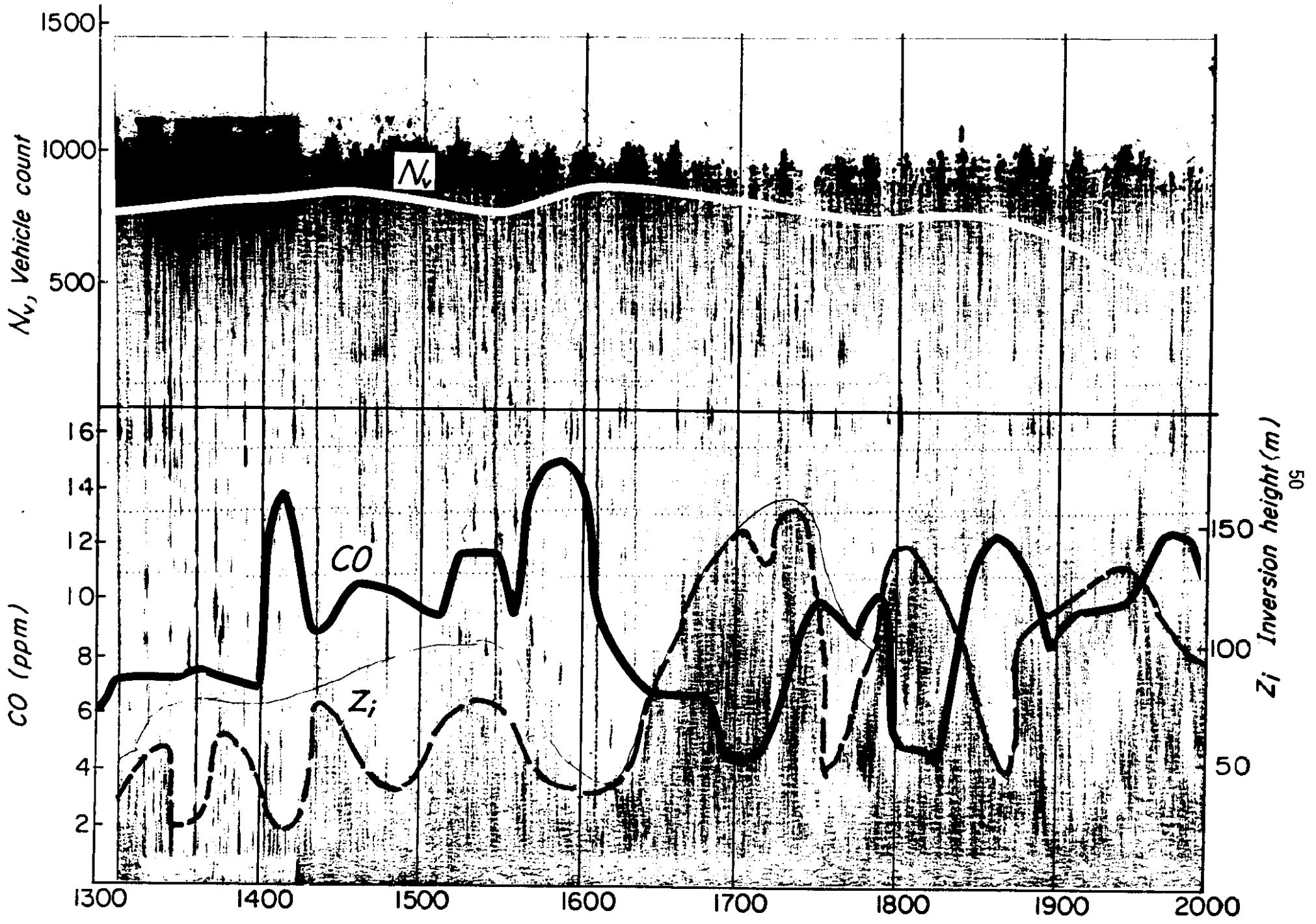

Figure 14. Acoustic Radar Records 11.20.76

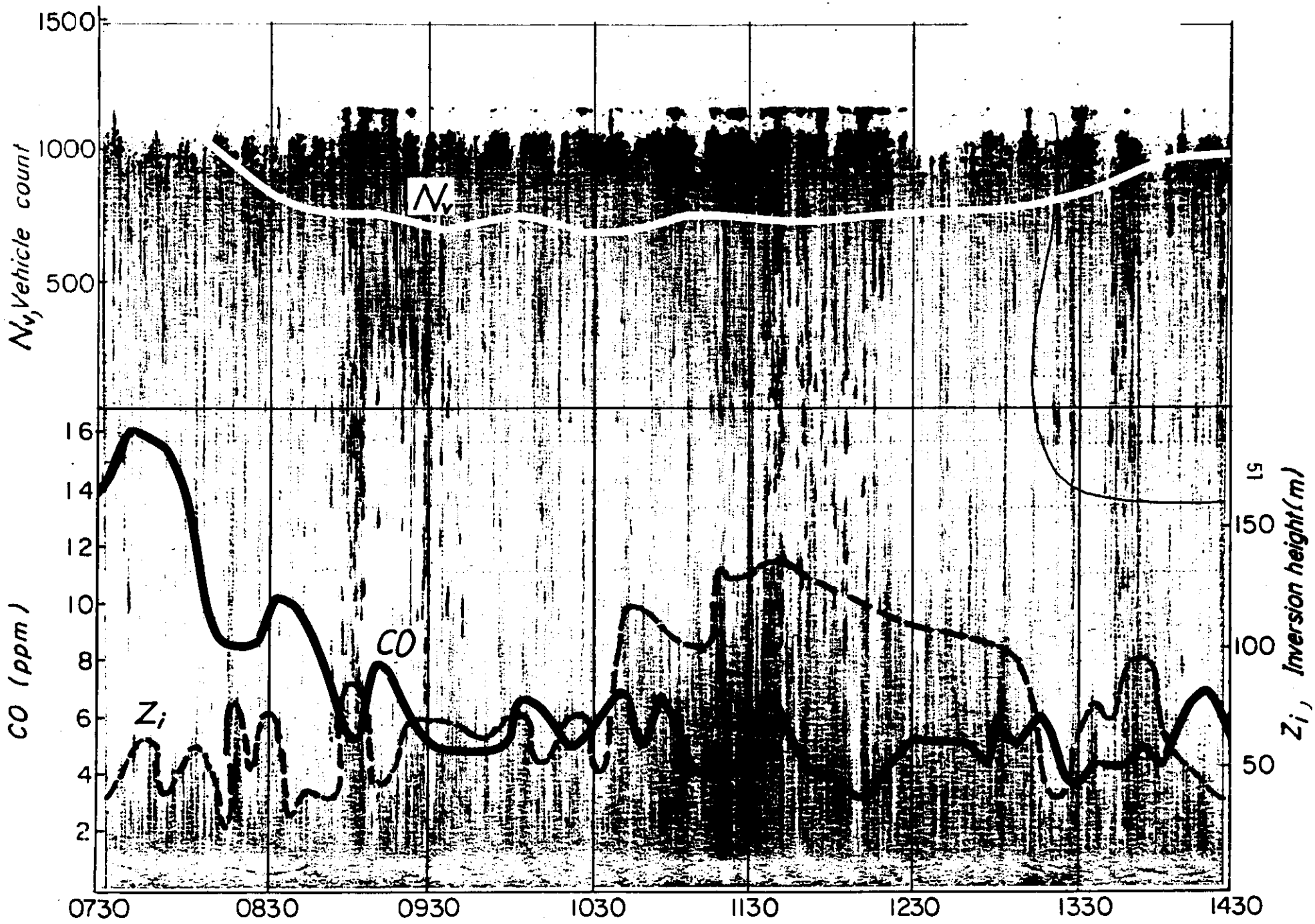

Figure 15. Acoustic Radar Records 11.22.76

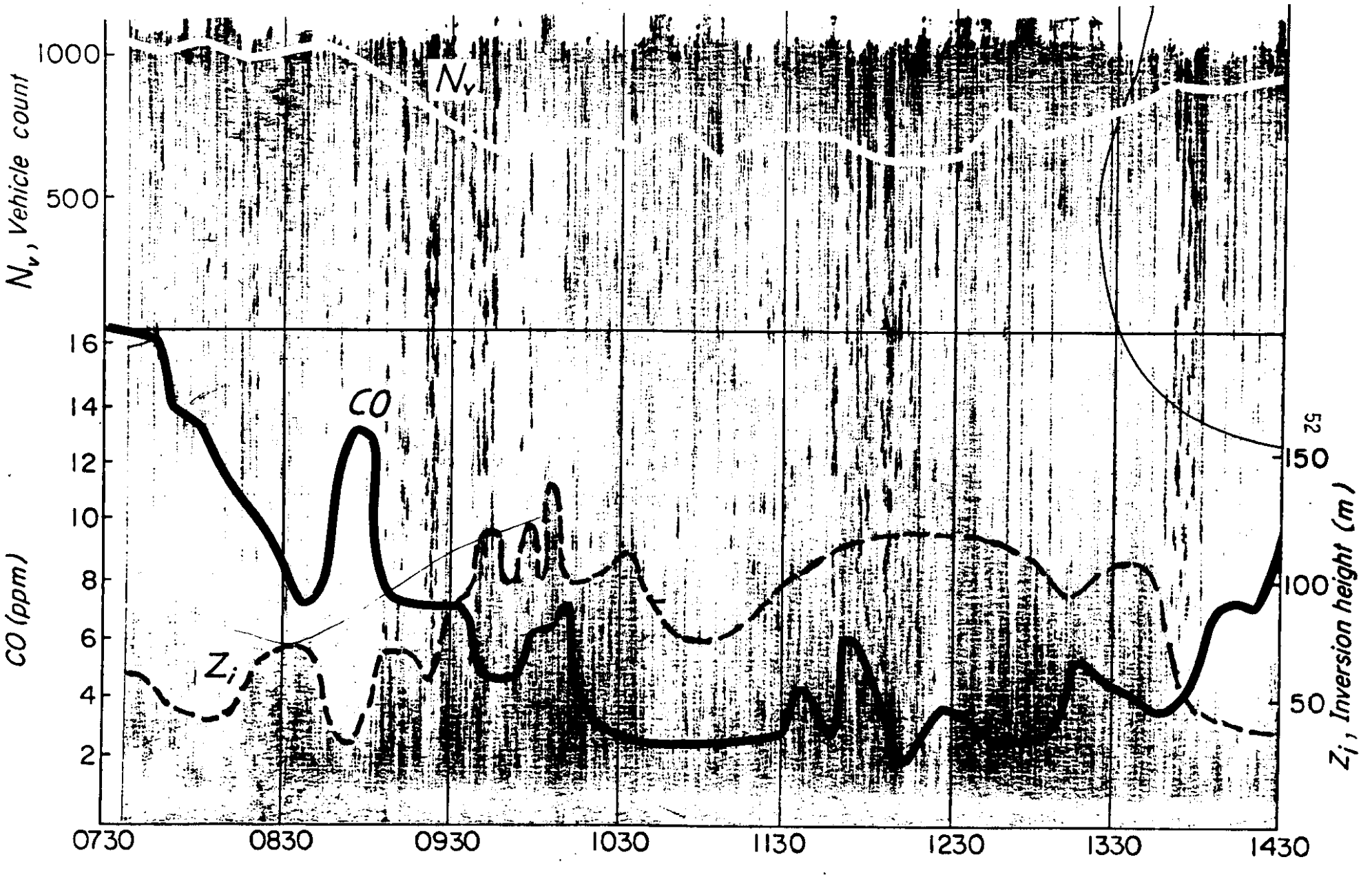

Figure 16. Acoustic Radar Records 11.23.76

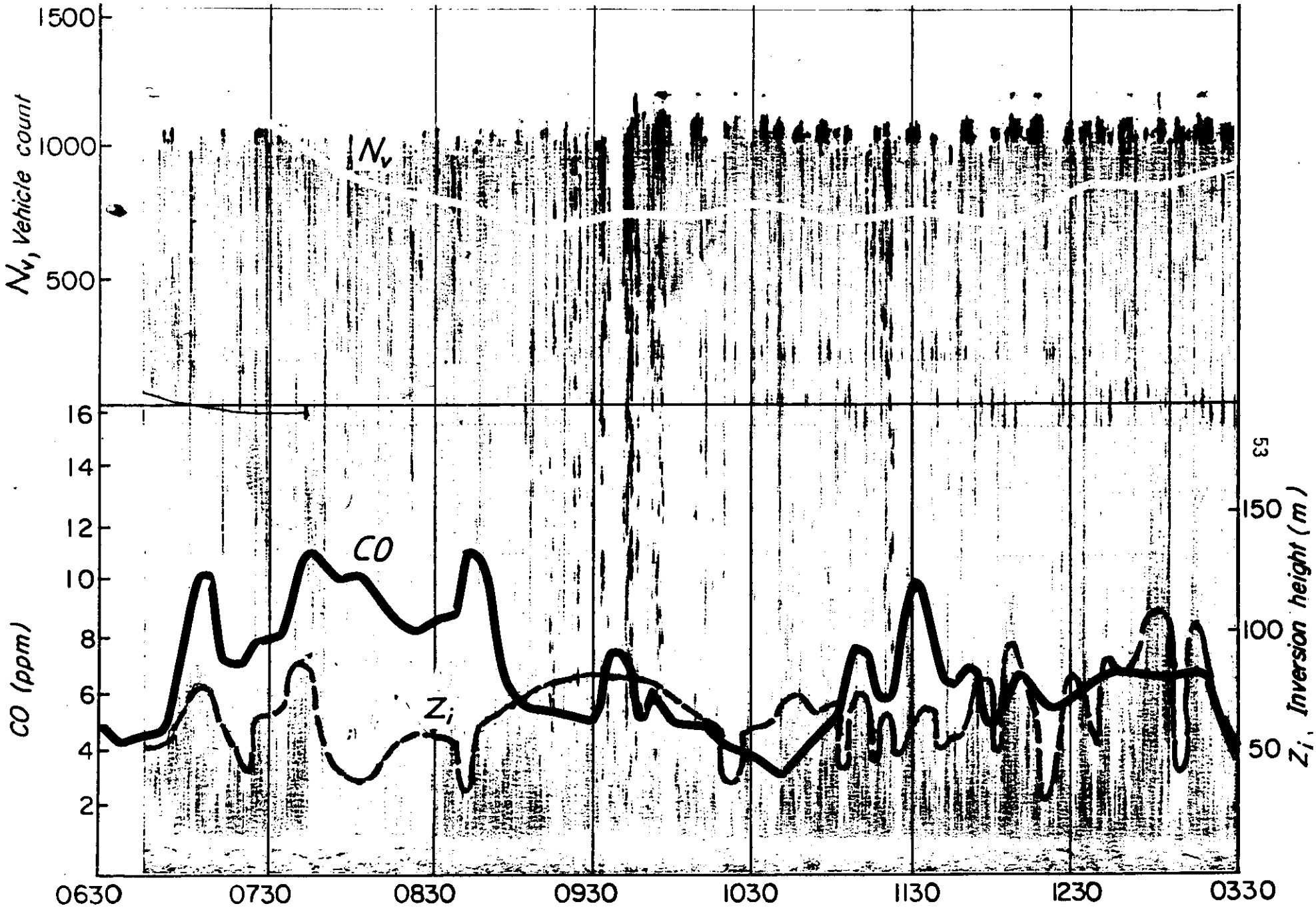

Figure 17. Acoustic Radar Records 11.29.76

Analyzing the characteristics of the N_V, CO, and N_i curves in Figures 12 through 15 two conclusions can be drawn:

1. There is an indication of a correlation between Acoustic Radar measured inversion heights (Z_i) and CO concentration.

2. The relation is negative in nature; that is, the CO concentration level is increasing with decreasing inversion layer heights.

The degree of association between CO concentrations and inversion heights was determined by the Pearson product-moment correlation coefficient, r(19). The formula used for developing this coefficient (r) is shown in Equation 3.

A correlation coefficient indicates the degree to which variation (or change) in one variable is related to variation (or change) in another.

$$r = \frac{\sum_{i=1}^{n} (Xi - \overline{X})(Yi - \overline{Y})}{\left\{ \sum_{i=1}^{n} (X_i - \overline{X})^2 \sum_{i=1}^{n} (Y_i - \overline{Y})^n \right\}^{\frac{1}{2}}} \qquad \text{(Equation 3)}$$

where r = correlation coefficient

X_i = Individual CO concentration data, (ppm), measured by samplings

Y_i = Individual inversion height value, (m), from radar records

$\overline{X}$ and $\overline{Y}$ are sample means derived by

$$\overline{X} = \frac{1}{n} \sum_{n=1}^{n} X_i \text{ , and} \qquad \text{(Equation 4)}$$

$$\overline{Y} = \frac{1}{n} \sum_{n=1}^{n} Y_i \qquad \text{(Equation 5)}$$

i refers to one individual sampled data of n number of sampled pairs (X_i,Y_i) correlated by Equation 3.

The measure of correlation (r) should assume only values between -1 and +1. Both extremes (+1, -1) indicate strong correlation. The correlation is positive when increasing one variable (X) results in increased value of the other one (Y). Correlating CO concentration and inversion heights the correlation factor is negative indicating that larger inversion height values are associated with lower CO concentration levels.

The correlation between CO concentration and inversion height is evaluated in Figures 18 and 19. Figure 18 correlates one hour average data collected during the rush-hour traffic period on November 22, 23, and 29, 1976. In Figure 19 continuous measurements were compared and averaged also for one hour intervals between 0730 and 1430 as depicted in Figures 17 through 19.

The degree of association in both sets of data indicates a reasonable correlation. With an increase in height of the inversion there is a decrease in CO concentration. Most sample periods were associated with low wind and high stability condition and indicate a good correlation of CO values and mixing for worst case conditions.

In both figures a linear regression line was determined to provide an analytic meaning of the widely scattered variables. This straight line is described by formula

$$Y = b + mX, \quad \text{where} \qquad \text{(Equation 6)}$$

X and Y are variables, b is called the intercept (on the CO ordinate) and m is the slope of the regression line, often called the regression coefficient. The values of r, m and b are given in Figures 18 and 19.

5.3 Comparison of Pasquill-Turner and Acoustic Radar Stability Determination Methods

Atmospheric stability is discussed in Chapter 3.1. It was pointed out that negative lapse rate or inversion, when the temperature of air increases

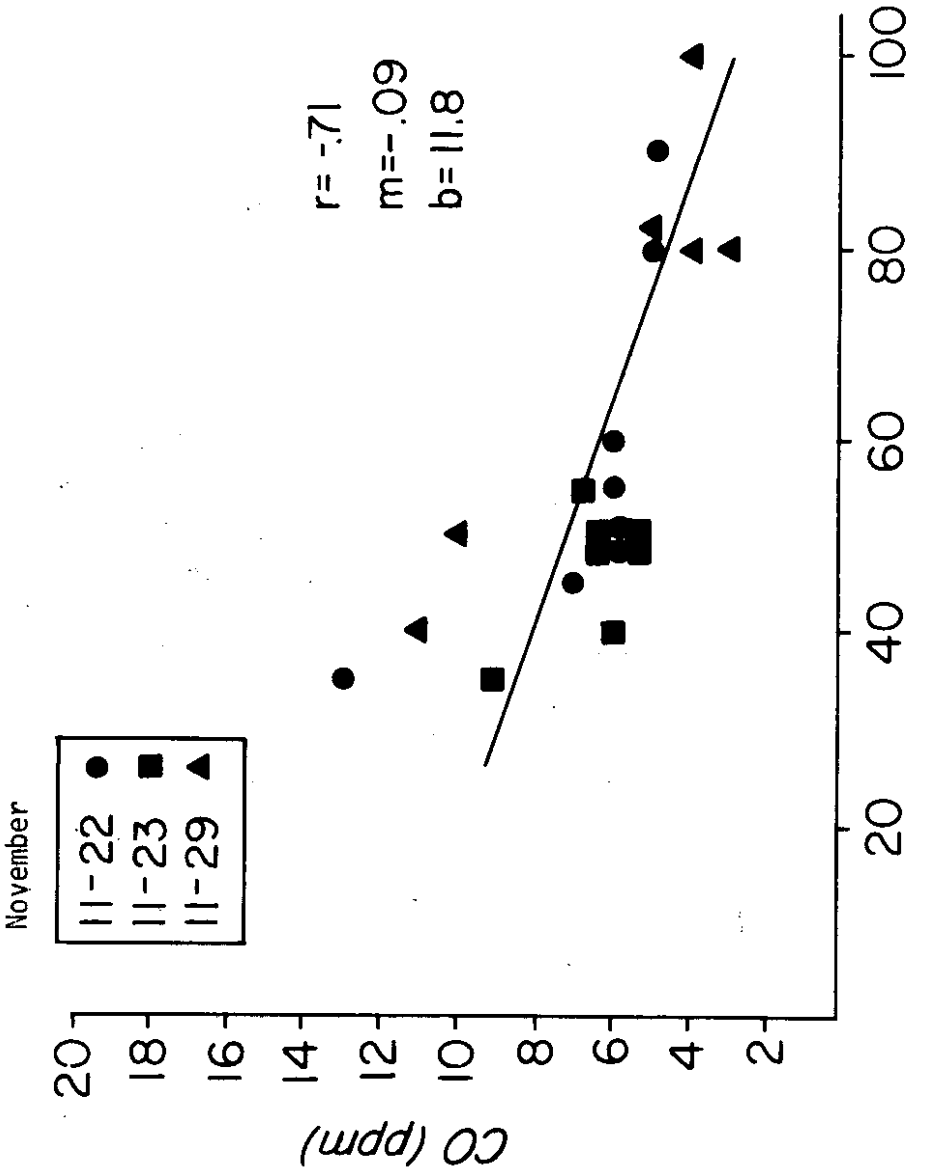

Figure 18. Inversion Height and CO Correlation

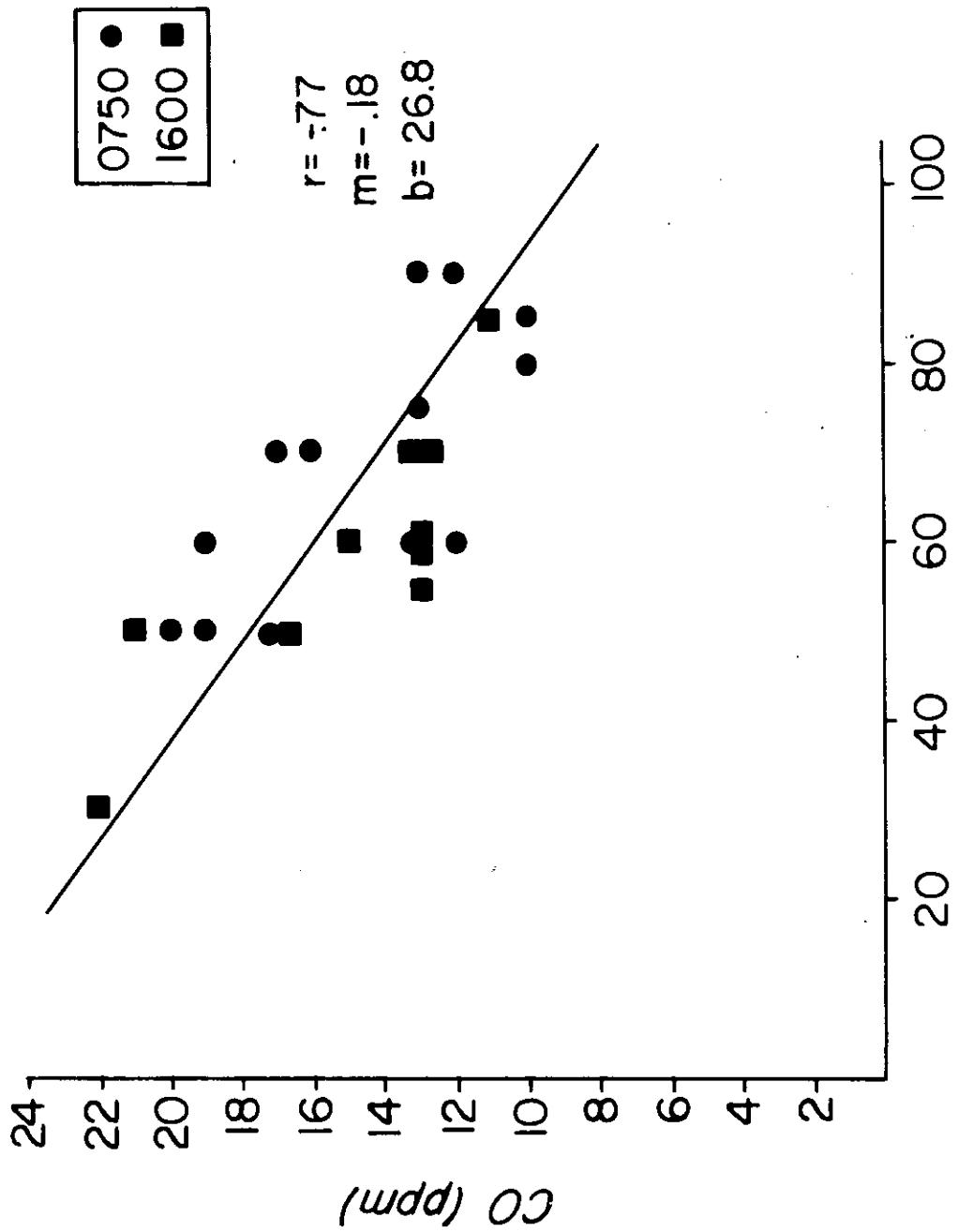

Figure 19. Inversion Height and CO Correlation

with increasing altitude, stabilizes the natural convection of air (vertical motion). The atmospheric condition became stable and the pollutants are trapped below the inversion layer. The lower the inversion height the higher the pollutant concentration level. The worst case is when the inversion starts on the surface of the earth. On the other hand positive lapse results in air convection, turbulences and unstable conditions with good dispersion of pollutants vertically and horizontally. At unstable conditions the pollutant concentration is low. Since the atmospheric stability reflects the pollutant concentration, it is a useful parameter in air quality prediction modeling. Pasquill categorized stability conditions into six groups denoting with E the most stable or worst condition and A the most unstable air. Turner interpreted the stability conditions and correlated them with such atmospheric parameters as wind speed, cloud coverage and solar radiation intensity.

The Pasquill-Turner stability determination method is based on an empirically developed classification using measured wind data and observed sky condition. This method is discussed in Chapter 3.2. The Acoustic Radar stability derivation method is discussed in Chapter 3.3.

The monostatic Acoustic Radar measures the atmospheric structure by echoes or acoustic waves scattered by temperature inhomogeneities in the atmosphere. This temperature microstructure field is caused by mixing across a non-neutral temperature gradient (adiabatic lapse rate is neutral temperature profile). The two types of echoes are thermal and shear echoes. Thermal echoes are formed in unstable air layers when the mixing is caused by thermal convection. Shear echoes are generated in air layers where the mixing is caused by wind shear. The base of the echo trace is the mixing height, the top is the inversion height (see Figures 7 and 8). To be able to correlate the two stability derivation methods, the echo traces were interpreted in terms of Pasquill stability classes. Thermal echoes are signs of

unstable atmospheric conditions class A and B; while shear echoes, which measure the height of the mixing and inversion layers, are more the indicators of stable conditions. Shear echoes at low altitude represent class E, and when the echo traces start at the terrain the stability is identified as F class in the Pasquill stability category.

For air quality studies stability classes D, E, and F, which are associated with high concentration levels, are of the most interest; whereas A, B, and C classification are of lesser importance in air pollution determination.

5.3.1 Previous Comparisons

Stability classification derived from Acoustic Radar data has been reported by Carsey et al by analyzing the data based on 1-hour averages (Appendix A). By comparing the various stability determinations, it was found that the Acoustic Radar derived mixing layer height was at least a reasonable indication of stability class. A comparison of stability classes derived by the Acoustic Radar and by the Pasquill-Turner Method are illustrated in Figure 20 based on this study (6). The stability classes in Figure 20 show a general trend of similarity, but deviate from each other in several instances. In some cases the Acoustic Radar data are higher and in other cases lower than the stabilities derived by the Pasquill-Turner Method. Figure 20 also shows a curve of the corresponding CO concentrations. Note that high CO concentration levels correspond with very stable atmospheric conditions.

Tombach and Chan investigated the correlation of mixing height and inversion height estimates from Acoustic Radar records and in situ temperature soundings (7). High degree of correlation was found between data generated by these different methods. It was concluded in this report that the Acoustic Radar could provide sufficient data on mixing and inversion heights for air quality modeling purposes without the expense and complexity of temperature soundings.

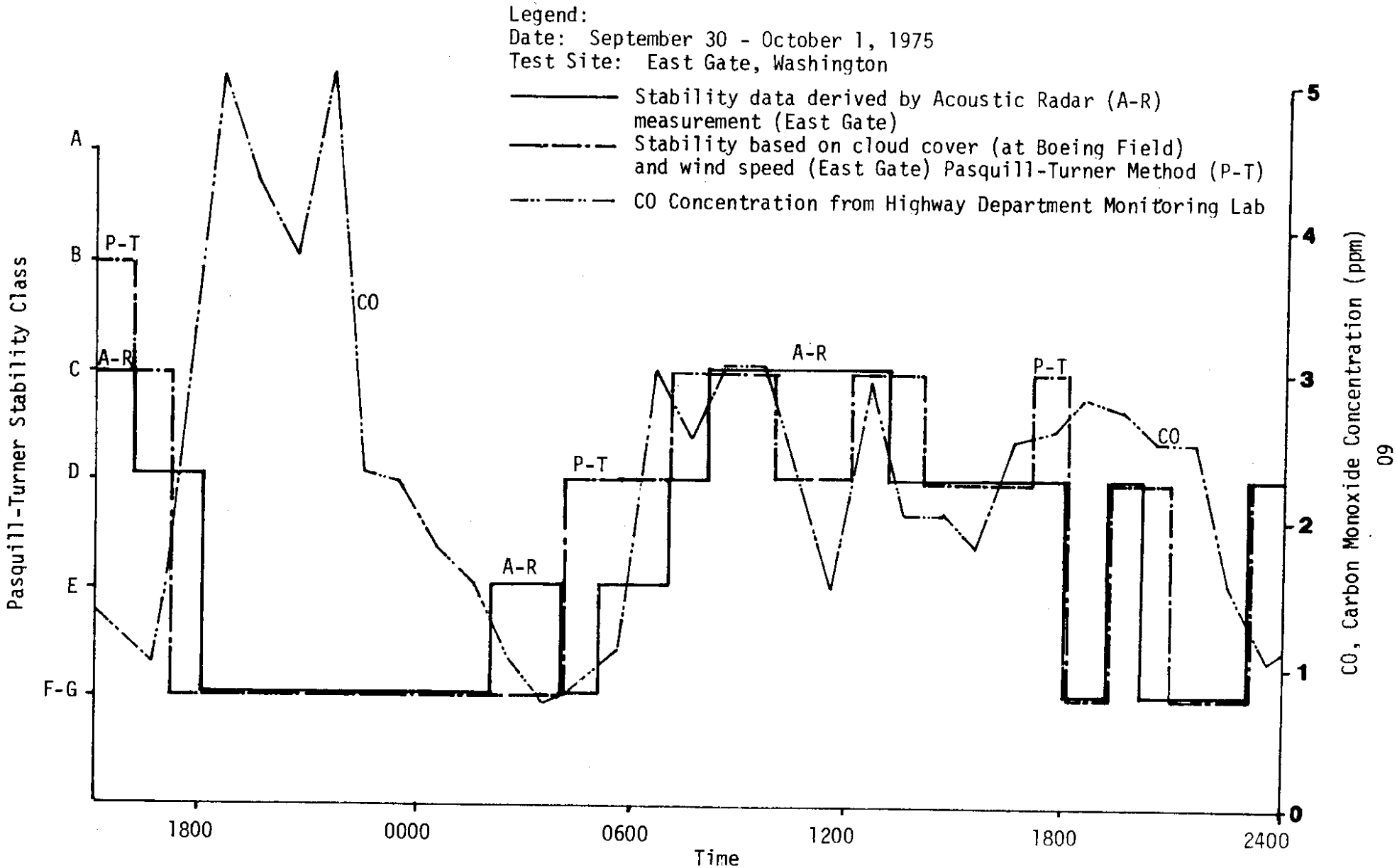

Figure 20. Comparison of Stability Classes Determined by Pasquill-Turner Method (P-T) and from Acoustic Radar Records (A-R) (9).

5.3.2 Comparison of Study Results

Over 60 atmospheric radar measurements were conducted for the purpose of comparison during the six week period between 11-1-76 and 12-15-76. Stability data measured during rush-hour conditions between the hours 0730-0830 and 1600-1700 were averaged over one hour periods. Stability classifications were also derived for the same one hour intervals from wind speed records and observed cloud cover using Pasquill-Turner Method. The derived stability classes as well as the meteorological data are charted in Appendix G. The frequency of occurrence of stability classes derived by both Pasquill-Turner and Acoustic Radar methods were compared in Figure 21. The results were in good agreement in the worst case (stability class F) and for unstable condition (stability class C). In the neutral category of D the Pasquill-Turner Method recorded 73.2% as opposed to 35.7% derived from radar data. The results for stability class E were just the opposite. Radar echoes show 41.1% E stability but only 3.5% E classes were derived by the Pasquill-Turner Method. The different percentage of E and D stability classes derived by Pasquill-Turner and radar methods can be explained by the characteristics of these derivation methods. Since all data were collected within one hour of sunrise and sunset, under the Pasquill-Turner Method they were categorized as nighttime variables. In the Pasquill-Turner Stability Method during nighttime periods solar radiation is not present and only two cloud cover conditions are defined. The reduced number of atmospheric parameters introduce some uncertainty in the determination of stability classes between categories of neutral stability (D) and moderately stable conditions (E). Radar echoes on the other hand reflect the atmospheric structure equally day or night. For this reason in most stable conditions (D & E) that is when low level inversions are associated with low wind speeds, the Acoustic Radar method appeared to be the better determinant of these stability classes. This observation was supported by Figures 18

and 19 which also show continuous variation of CO concentration and mixing height variation in conflict with the ragged stability population of the Pasquill-Turner Method in Figure 21.

5.4 Error Analysis

There are several sources of error that might have influenced the final results of this study. They can be grouped into three categories; instrument, sampling, and human errors.

Instrument and sampling errors may include:

1. Valve and pipe leakage: leak tests were performed regularly, but it was difficult to determine whether or not there were small leaks in the approximate 1000 feet of 3/4 inch PVC piping.

2. Interferences: a sample stream may contain, in addition to carbon monoxide, various other infrared absorbing substances. Common interferences are CO_2, SO_2, CH_4, H_2O, and Hexane. These interferences were kept to a minimum by desiccant placed in the reference cell.

3. Inaccurate zero and span of the Analyzer: this may have occurred due to the calibration of the gases, or their change in concentration over the time period of the study. This error is at most 2 ppm.

4. Poor adjustment of Acoustic Radar read-out: it is possible to change the contrast of the sounder record, to optimize signal readings. If records were too dark the contrast was decreased, which might have eliminated a weak signal. Also the height zero was adjusted with an approximate method which introduced an error of $\pm$ 5 meters.

Human errors may include:

1. Inaccurate reduction of data:

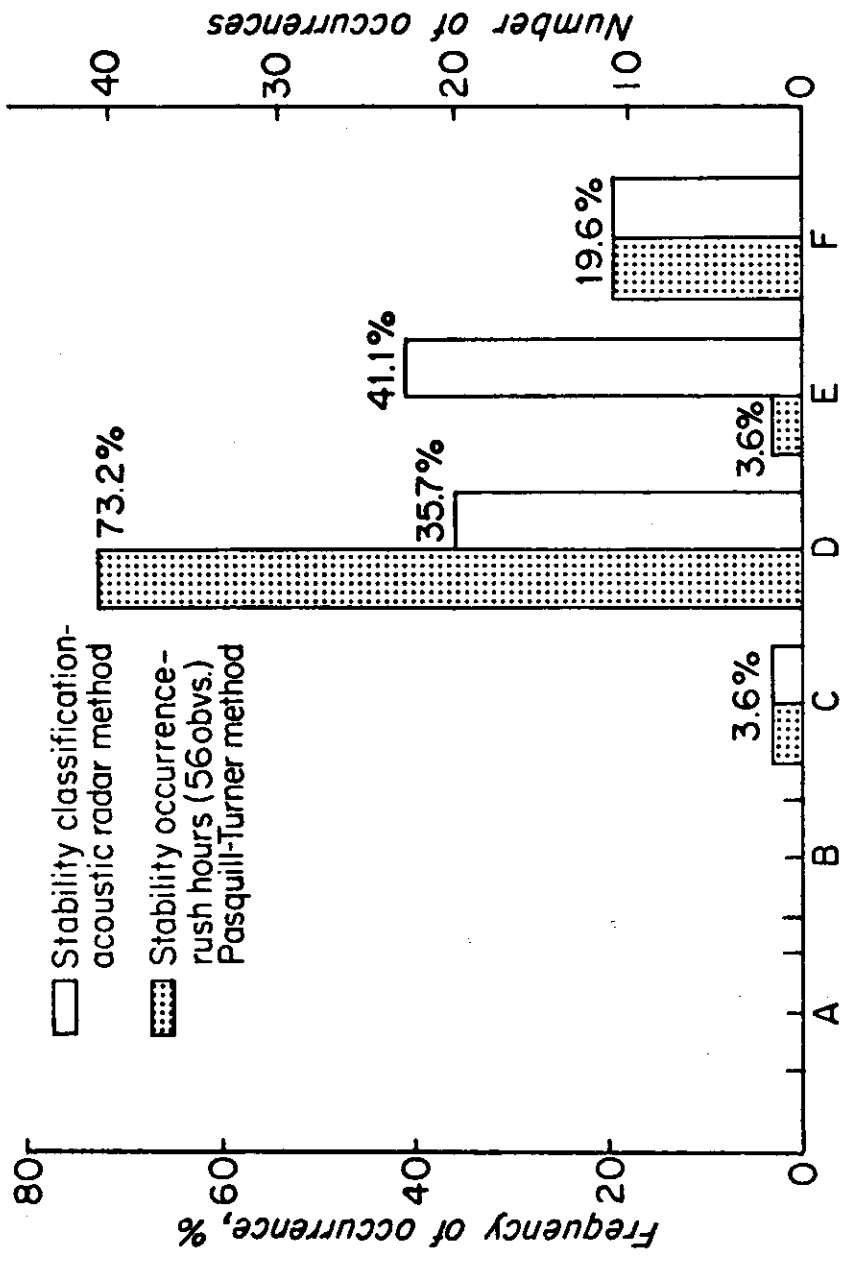

Figure 21. Frequency of Stability Class

a. Error in visual averaging of CO concentration records was kept to a minimum by reducing three minute increments which represented each side of highway. Error is estimated at $\pm$ 2 ppm.

b. Visual reduction of Acoustic Radar data, involved averaging short-term variation. In determining one hour averages error is estimated at $\pm$ 5 meters.

c. Error in reducing and interpreting low wind speeds, which were a characteristic of the study period. The instrument used is only reliable at wind speeds above 2 mph.

2. Inaccuracies in determining stability classification: Determination of atmospheric stability categories by the Pasquill-Turner Method is fairly subjective, because of estimates in the cloud cover fraction and height. Accurate information may be obtained from local weather stations (airports), but these data are collected at the specified sites, and may not be representative of the study area. This information is compiled only at one-hour intervals.

3. There are limitations in the applicability of the HIWAY model with respect to this study. In particular, under "worst case" conditions, (conditions of extreme stability, very low wind speed and variable wind direction), the model tends to overpredict. Equation 2 shows that as the wind speed approaches zero, Q gets very large, which will invalidate the model. Most of the monitoring in this study was conducted under "worst case" conditions where the EPA-HIWAY model does not provide reasonable values.

6. Conclusions

1. The findings of this research demonstrate the fact that Acoustic Radar provides a descriptive picture of atmospheric structure, continuously both day and night. Radar echo measurements represent a more direct indication of stability conditions than the Pasquill-Turner method for empirically determining stability categories, especially D and E. This fact is particularly important in evaluating stability during critical nighttime periods, as well as sunset and sunrise, when increased motor vehicle emissions and atmospheric stagnation generally occur.

2. A comparison of radar and carbon monoxide monitoring data showed that inversion height as determined by radar echoes was inversely related to carbon monoxide concentration.

7. Implementation and Recommendations for Future Research

The results of this study indicate that the Acoustic Radar could be a valuable tool in air quality modeling for transportation sources for two reasons:

1. The radar echoes have been shown to be directly related to atmospheric stability and carbon monoxide concentrations.

2. The Acoustic Radar provides a continuous record both day and night.

The results of this research could be implemented in the following ways:

1. Utilize Acoustic Radar data for determining stability categories in lieu of the Pasquill-Turner method, in modeling based on gaussian diffusion. This should result in more accurate predictions for the D and E stability conditions, and nighttime periods when continuous radar data are available. This is especially important since critical air quality conditions are associated with high motor vehicle emissions and atmospheric stagnation, both of which generally occur at sunset, sunrise and at night.

The following recommendations for future research are offered:

1. The findings that carbon monoxide concentrations can be directly estimated from radar echoes suggests the possibility of developing a predictive model which would be simpler and more reliable than the currently used gaussian diffusion models. Therefore it is recommended that systematic research program be undertaken to find the relation between Acoustic Radar derived atmospheric parameters and concentrations. The objective would be to develop a simpler technique for air quality prediction for transportation sources.

2. As a by-product of this study it was found that queuing of motor vehicles as a result of traffic congestion is a major contributing factor to carbon monoxide concentrations. It is recommended therefore that a

more detailed study be undertaken of the effect of queuing on carbon monoxide concentrations. This should lead to the development of improved models for determining carbon monoxide emission patterns. Such a tool would provide improved emission input data for air quality diffusion modeling, leading to more accurate predictions of carbon monoxide concentrations.

References

1. User's Guide for HIWAY, A Highway Air Pollution Model, EPA Publication No. 650/4-74-008, 1975.

2. Rossano, August T., et al., The Selection and Calibration of Air Quality Diffusion Models for Washington State Highway Line Sources, W.S. Highway Dept. Research Program Report 12.2, 1975.

3. Rossano, August T., A Critical Review of Mathematical Diffusion Modeling Techniques for Predicting Air Quality with Relation to Motor Vehicle Transportation, Washington State Department Research Program Report 12.1, 1973.

4. Pasquill, Turner, Deriving Stability Class, Journal of Applied Meteorology, February, 1964.

5. Turner, D. B., Workbook of Atmospheric Dispersion Estimates, Public Health Service Publication No. 999-AP-26, 1969.

6. Carsey, Frank; Lamb, Donna V.; Badgley, Franklin I.; Rossano, August T.; Alsid, Hal; An Examination of the Feasibility of Using an Acoustic Sounder for Air Pollution Studies, University of Washington, 1976.

7. Tombach, Ivar; Chan, Michael; Aerovironment Inc., Estimation of Mixing Depth and Inversion Height by Acoustic Radar - A Comparison with In-situ Measurements, 17th Conference on Radar Meteorology, 1976.

8. Elias, D., and Robinson, E., The Relationship of Acoustic Sounder Records to Pollutant Levels in Connecticut, Washington State University; Presented at the 69th Annual Meeting of the Air Pollution Control Association, July, 1976.

9. Hall, Freeman F., Jr., Temperature and Wind Structure Studies by Acoustic Echo-Sounding, NOAA, 1973.

10. Supplement No. 5 for Compilation of Air Pollutant Emission Factors, EPA Publication No. AP-42, 1976.

11. Juhasz, Paul C., Development of a Carbon Monoxide Traffic Emission Density Pattern for the Bellevue Business District, a Master's Thesis, University of Washington, 1977.

12. Tombach, Ivar; Macready, Paul B.; Baboolal, Lal; Aerovironment, Inc., Use of a Monostatic Acoustic Sounder in Air Pollution Diffusion Estimates, ISA JSP6677, 1973.

13. Rossano, August T., Evergreen Point Bridge Toll Booth Ventilation Study, Washington State Highway Department Research Program Report 4.1, 1972.

14. Operating Manual for Model 315B Infrared Analyzer, Beckman Instruments, Inc., 1971.

15. Meteorological Factors Affecting Atmospheric Pollutants, EPA Training Course Manual, 1974.

References(continued)

16. Interim Operating Instructions, Model 300 Acoustic Radar, Aerovironment, Inc., 1974.

17. Szepesi, Dezso J., "Application of Meteorology to Atmospheric Pollution Problems on a local and Regional Scale", Commission for Special Application of Meteorology and Climatology(CDSAMC), final report, April, 1977.

18. Boys, Paul A., Investigation of Carbon Monoxide Dispersion from a Line Source, a Master's Thesis, University of Washington, 1975.

19. Feigl, Polly; Ipsen, Johannes, Bancroft's Introduction to Biostatistics, New York, 1970.

20. Chock, David P., General Motors Sulfate Dispersion Experiment: Assessment of the EPA-HIWAY Model, Journal of the Air Pollution Control Association, Vol. 27, No. 1, January 1977.

21. Department of Environmental Quality, Oregon, memo.

Appendices

Appendix A

Executive Summary

AIR QUALITY MODELING - PHASE 2

Frank Carsey
Donna Lamb
Frank Badgley
August Rossano
Hal Alsid

July 14, 1976

University of Washington
Seattle

Essentially, the device worked satisfactorily. Comparison of the Model 300 to research radars (largely produced by NOAA) showed that far better data accessibility was possible than with the Model 300. A small pulse repetition rate and an under-designed writing amplifier are evident. Also, electronic filtering in the Model 300 is apparently not as effective as is possible. A very important element lacking in the Model 300 is a simple way to "zero" the instrument. It is difficult to set the tone burst in synchronization with the placement of the writing stylus at a given point on the record. This difficulty alone accounts for more than 10 m of error in measuring heights. In the course of a year's operation it was necessary to adjust some internal variable resistors and replace two sets of bearings. The latter maintenance points up the need to clean out the recorder area, preferably with a small vacuum cleaner, about once per week. The basic durability of the instrument is not a problem; the design of the instrument restricts its full utilization.

III. Site Descriptions

A. Puget Power Site - Sedro Woolley, Washington

The first site, in Sedro Woolley, Washington was chosen because of the meteorological tower located there in conjunction with the Puget Power Nuclear Site. The tower was equipped with instruments at three levels that allowed a comparison of the acoustic sounder echoes with the more traditional meteorological variables, particularly in the lowest levels of the atmosphere. Since the instrument was specifically designed to look at these levels, it was desirable to verify that it could, indeed, sample these levels.

After some preliminary tests at the University of Washington campus and the construction of the antenna, the sounder was installed at the Sedro Woolley site on July 31, 1975 and operated there until about September 15, 1975. The

sounder was located approximately 200 feet to the northwest of the meteorological tower in the middle of a gently rolling pasture. The site is located on a plateau above the flood plain of the Skagit River on the north side of the valley. To the north of the site the foothills rise above the plateau. The Puget Power people were most cooperative in allowing the use of part of their instrument shelter next to the tower for our recording equipment.

The tower itself is approximately 210 feet high with instruments at 65 feet, 110 feet and 200 feet. Wind speed and direction are measured at the top and bottom levels and are recorded on continuous strip chart recorders. Wind speed is also clocked at each mile of rotation for averaging very low wind speeds. The wind direction sensor at the bottom level is also tied in to a sigma computer to record the standard deviation of the wind direction with time. The temperature sensors were located at each level. The bottom included a reference temperature and a temperature difference probe matched with one at the top to obtain the differential temperature. Similarly, a pair of sensors was located at the middle level and the bottom to measure that temperature difference. The output from the reference and two ΔT's were recorded by a multipoint strip chart recorder. A time lapse camera located in the river valley and looking north eastward at the site was utilized to verify conditions of fog and rain.

The first several weeks of sounder data were used to verify the reactions to different settings of the instrument. The weather included many rainy days during this period and only a few strong nocturnal inversions. Later in the period there were better inversions. The last week that the sounder was on site there were problems with some of the meteorological instruments on the tower. Usable temperature difference data ended on approximately 8am EST, September 11.

Other than the large number of person hours necessary to retrieve useable averages from the strip charts, the sounder and meteorological data are reliably of good quality and allow some good comparisons between the two means of sampling the atmosphere. In particular, it is soon clear that the sounder also sees what is happening between the instrumented levels on the tower. The sounder trace can be seen to be related to ΔT, a traditional indicator of atmospheric stability. This is discussed further in Section IV.

B. Eastgate, Washington

At the second site the acoustic sounder was placed near the Washington State Highway Department monitoring laboratory that was monitoring near Interstate 90 in Eastgate, Washington. The objectives here included preliminary comparisons with the Pasquill-Turner method of determining atmospheric stabilities, assessing the instrument's vulnerability with respect to traffic noise, and preliminary attempts at correlating pollution concentrations with the sounder's echo.

The site was located in an east-west pass through the Sunset Hills. I-90 is located in the bottom of that ravine. The site was approximately one mile west of the I-90-148th Avenue SE interchange. The Highway Department trailer was located about 350 feet north of the northern most lane of I-90. The site was a vacant lot near some low office buildings and a trailer sales lot.

The sounder was set up on the site on September 26, 1975 and was operated until October 9, 1975 when the Highway Department trailer was moved.

The instrumented trailer records temperature, wind speed and direction at the 10-meter level and samples several atmospheric pollutants: carbon monoxide, total hydrocarbons, methane, non-methane hydrocarbons, nitrogen dioxide. The data were available as 1-hour averages of all variables and the strip

chart data for winds. Meteorological data from Boeing Field were obtained from the National Weather Service to allow the determination of stability conditions based on cloud cover and ceiling height which were not routinely recorded at the site.

With no concurrent traffic data the data must be stratified into day of the week in order to be able to compare essentially the same source strength at different meteorological conditions. The period of record was not long enough to do this. The data also must be stratified to some degree by wind direction and again the statistical sample was not great enough. The 1-hour averaging time imposed by the data is too restrictive for the preliminary evaluation of the sounder data. A longer period of record at an air quality monitoring site was desirable.

C. Duwamish Site

The air quality monitoring site operated by Seattle City Light was chosen as a third location. It is located in the Duwamish river valley across the river, but near the south end of Boeing Field. The Duwamish Valley is noted for frequent and persistent temperature inversions that cause high pollution concentrations. It was felt that this more permanent site might yield some interesting stability patterns at night.

The sounder was located just outside of the Seattle City Light substation, approximately 100 yards to the west of the edge of the river and approximately the same distance north of the monitoring trailer. The site is basically flat with an open field to the north and some industrial development across the river to the east. The land is about 20 feet above the low tide mark of the river. There is a small rise to the southwest of the site representing the hills building up to the plateau that Sea-Tac is located on. The site is often in the flight path of either Sea-Tac or Boeing Field. The South Seattle

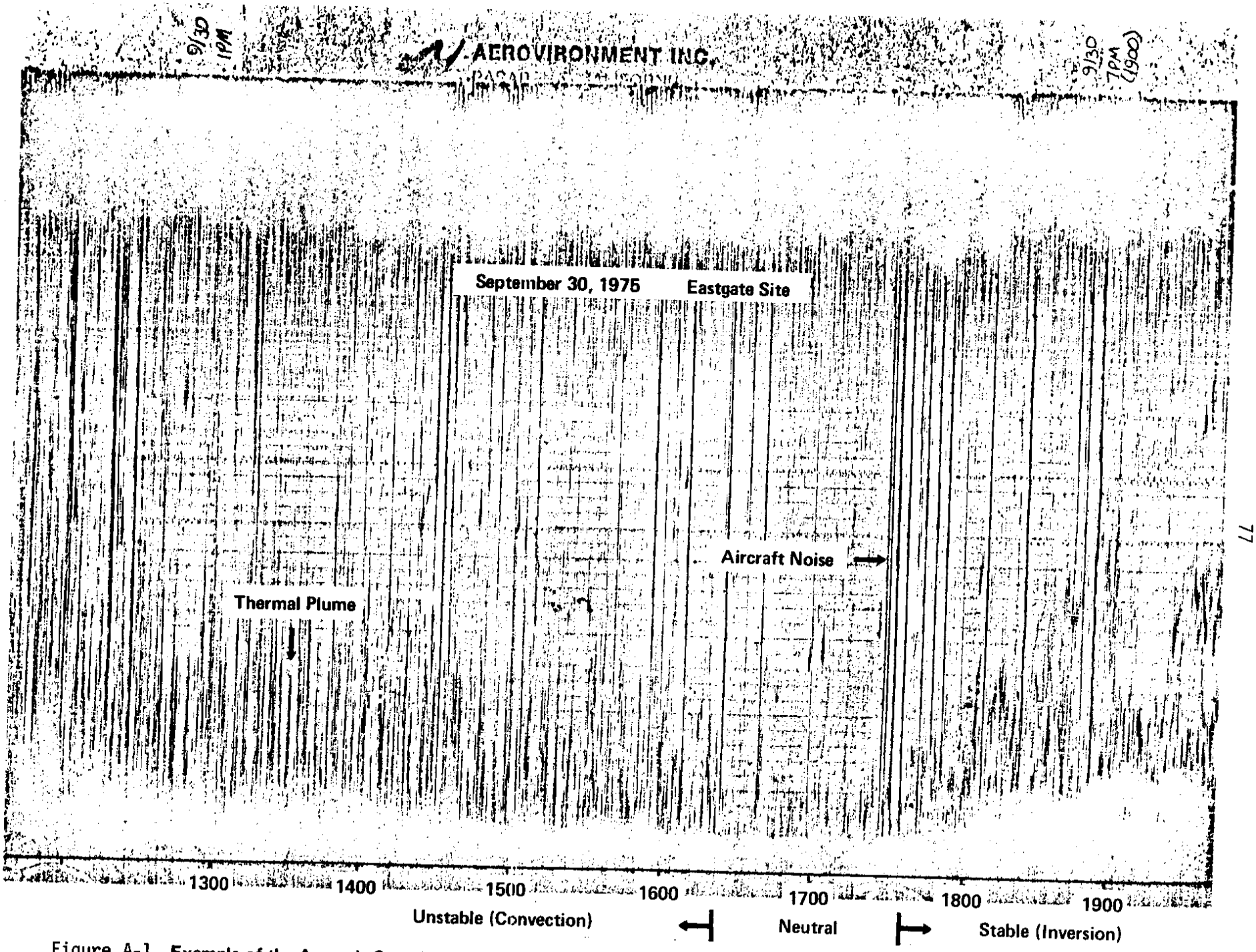

Figure A-1. Example of the Acoustic Sounder Record Showing Unstable, Neutral, and Stable Signatures, Thermal Plumes, and Aircraft Noise.

Freeway is located approximately 1/2 mile to the southwest of the site.

The sounder was set up on the site on December 19, 1975 after some negotiations to obtain power and permission to use the site. The air quality monitoring trailer on the site monitors many meteorological variables, as well as air quality data. The data is telemonitored to the Puget Sound Air Pollution Control Agency offices where the data is checked for instrument problems and is stored for computer analysis. The meteorological data include wind speed and direction at two levels and the temperature difference between the two levels. Air quality measurements include: nitrogen dioxide, nitrogen oxides, hydrocarbons-less-methane, carbon monoxide, sulfur dioxide, suspended particulates, and coefficient of haze.

The sounder data is noisy but good until approximately January 9, 1976 when problems with the recorder led to some data loss. There are some good days with subsidence inversion conditions in December as seen by the sounder, but the air quality and meteorological data is intermittent during this period. Carbon monoxide values are generally below 2 ppm during most of the rest of the period making comparisons not very clear.

IV. Comparisons between Meteorology and the Acoustic Sounder Record

The acoustic sounder records two distinct echo forms that generally allow easy recognition of unstable, neutral, and stable regines. Figure shows a typical (as opposed to a good) example of the transition from weak thermal plume activity in the afternoon characterized with the form often called "spikes" or "roots", to the neutral regime at sunset with little or no echoes visible, to the beginnings of the development of low level inversions with the signature that shows some evidence of waves and multiple layering and shows more continuity with time. (The vertical lines running from the top to the bottom of the trace come from aircraft flying overhead.)

Air pollution studies and modeling are not so often concerned with distinguishing between different stability categories under unstable conditions as under stable conditions. With this in mind, the approach has been to focus on looking primarily at the stable inversion data to attempt to distinguish between cases of moderate and extreme stability.

The first approach in interpreting the sounder record more carefully was to compare the sounder echoes with simultaneous temperature difference data available from the first site. Temperature variations in the vertical are an important way of determining the vertical mixing properties of the atmosphere. By measuring temperatures at different heights on-site, the localized effects on stability due to surface roughness changes, local valley or slope winds, or decreased mixing in a valley floor can be more reliably studied. Continuously recorded data may show more stability fluctuations than are implied by stability determinations from hourly observations.

The Atomic Energy Commission has established guidelines for relating temperature difference information to generalized stability classes A through G. These are summarized in Table A-1 as converted to the heights of the temperature sensors on the tower.

The continuous ΔT information was converted to the same size and direction for overlaying on the acoustic sounder trace. Figure A-2 shows one such overlay. Neither the ΔT between the top and the bottom of the tower, nor the ΔT between the middle and the bottom shows any clear correlation with what the acoustic sounder sees. The temperature difference between the

TABLE A.1 CLASSIFICATION OF ATMOSPHERIC STABILITY (AEC)

		tower ΔT top - bottom	tower ΔT middle - bottom
Extremely unstable	A	< -.9	< -.4
Moderately unstable	B	-.9 to -.8	-.4
Slightly unstable	C	-.8 to -.7	-.4 to -.3
Neutral	D	-.7 to -.2	-.3 to -.1
Slightly stable	E	-.2 to +.7	-.1 to +.3
Moderately stable	F	.7 to 1.9	.3 to .9
Extremely stable	G	> 1.9	> .9

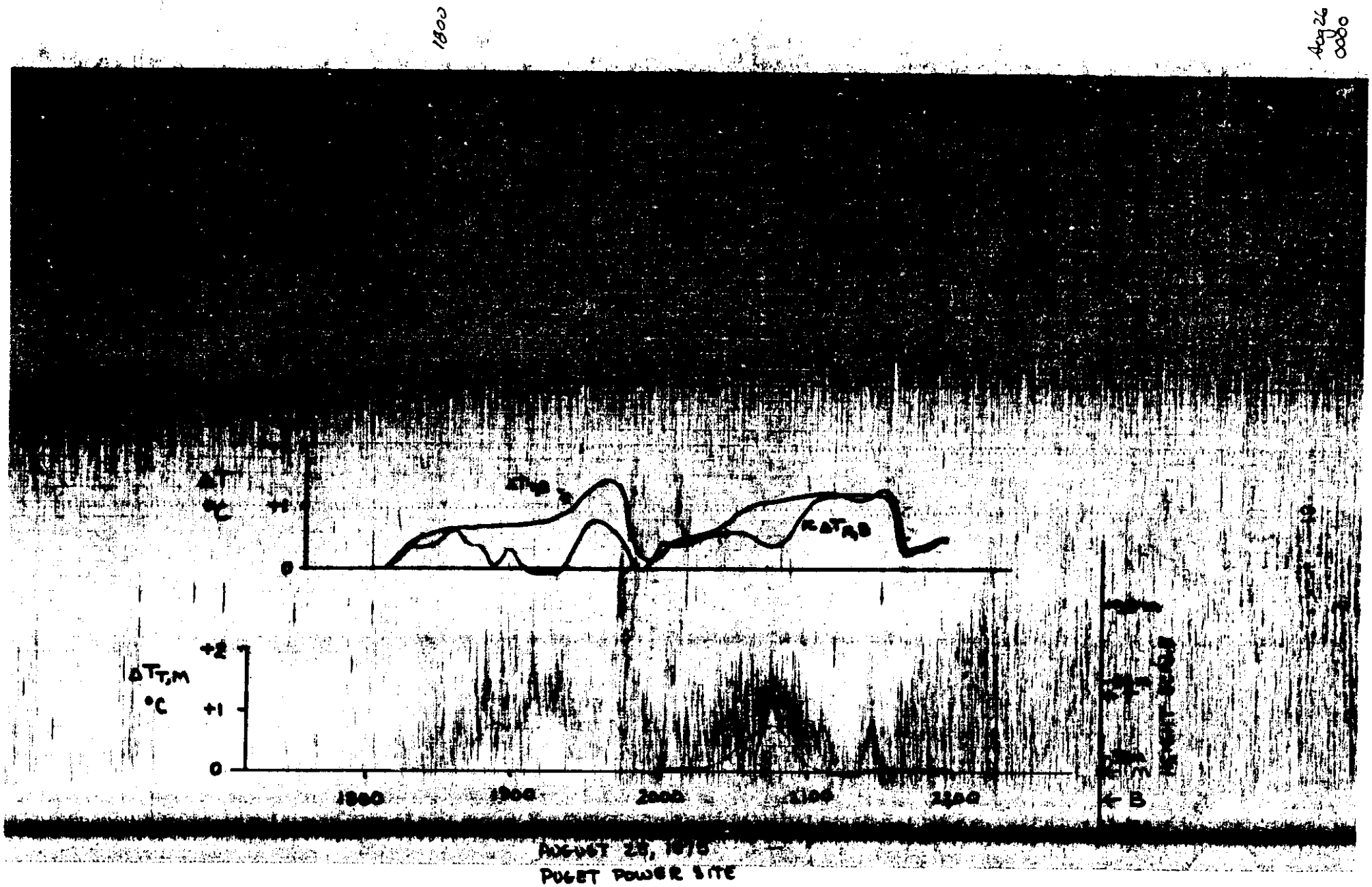

Figure A-2. ΔT Overlayed on Acoustic Radar Data

top and the middle of the tower was calculated and plotted on the same scale. This shows a good correlation. The height scale on the right hand side of the figure indicates the location of the tower sensors with respect to the sounder trace. Note that when the grey echo separates from the surface near 1915 that the ΔT between the middle and the bottom levels indicates more neutral conditions, while the ΔT between the top and the bottom indicates a strong inversion. This implies that there is mixing below a strong temperature inversion. At 2015 the inversion is located near the surface with neutral conditions above. These two times are illustrated in Figure A-3 with the temperatures plotted with respect to height.

Figure A-4 is another example of this analysis. Again, the sounder trace is returning information from heights as low as 25 meters and is representiative of the stability conditions between 30 and 60 meters. The inversion strength at these heights is often intensified when there is relatively more mixing lower down. Note the wave-like periodicity of these variations. The period is between 40 and 45 minutes between troughs.

The sounder is seeing short time scale variations in the stability and mixing characteristics near the surface. A potentially useful feature of the sounder is that it is more portable and less trouble than a tall permanent tower which is best for measuring ΔT's. It is of interest how the stability information of the sounder relates to the more classical definitions of stability using hourly weather observations.

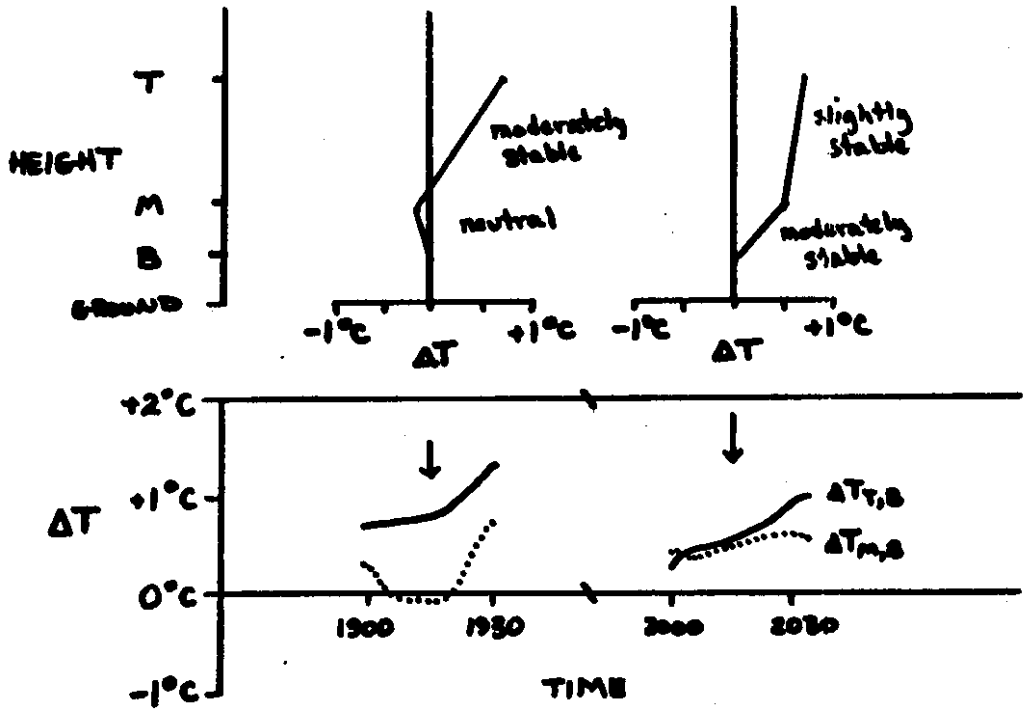

Figure 3. Two Examples of Temperature Difference Data Plotted as the Variation of Temperature with Height. August 25, 1975. Puget Power Site.

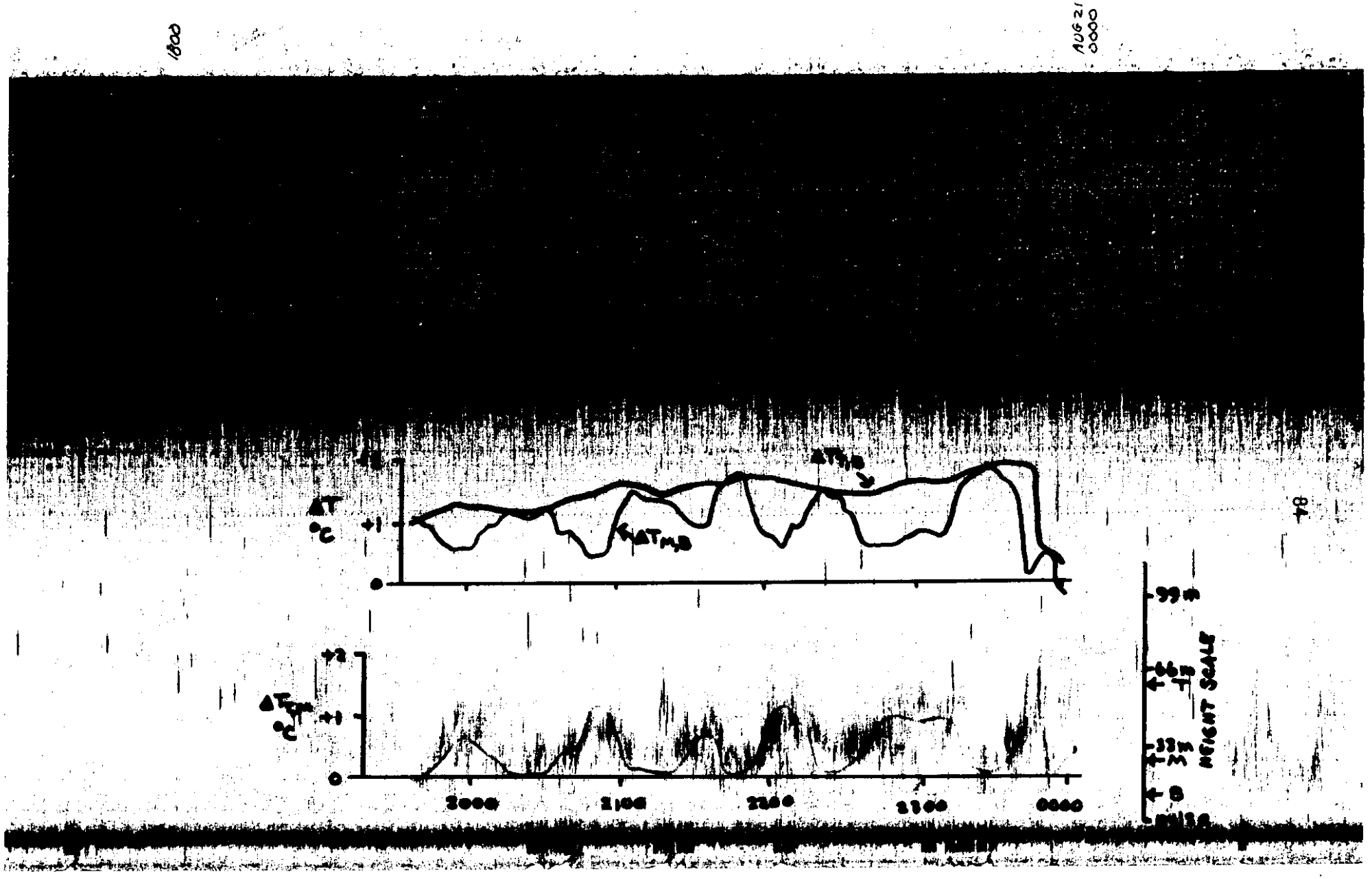

Figure A-4. ΔT Overlayed on Acoustic Radar Data

The Pasquill-Turner stability classification system uses hourly weather observations. The stability is dependent upon net radiation, which is influenced by cloud cover and solar incident angle, and wind speed. The procedure described by D. Bruce Turner in the February 1964 Journal of Applied Meteorology was followed using Boeing Field cloud cover and ceiling data. Wind speeds from the Eastgate monitoring trailer were used for the final determination of stability. These were plotted as a function of time as shown in Figure A-5.

For the acoustic sounder analysis, the record was analyzed based on a 1-hour average. Where the inversion extended all the way to the surface the hour was given F stability; where there appeared to be a mixing layer below the inversion the stability was designated as E. The distinction between neutral and unstable stabilities was also used. These results are also plotted in Figure A-5. The following Figure A-6 shows a portion of the sounder record. There are a few instances of lower level mixing, but they are of short duration. The sounder indicates that stable conditions persisted later in the morning hours at the Eastgate site in spite of winds picking up. Otherwise, the agreement is very good. The incidence of fog may explain the late onset of thermal convection.

Because of the spatial and time dependent nature of the source of carbon monoxide the development of a correlation between measured concentrations and stability parameters is more difficult. The relevant carbon monoxide concentrations are also plotted on Figure A-5. To correctly interpret the data it would be important to know the strength of the source (traffic volumes) concurrent to the monitoring time. Furthermore, the data would probably have

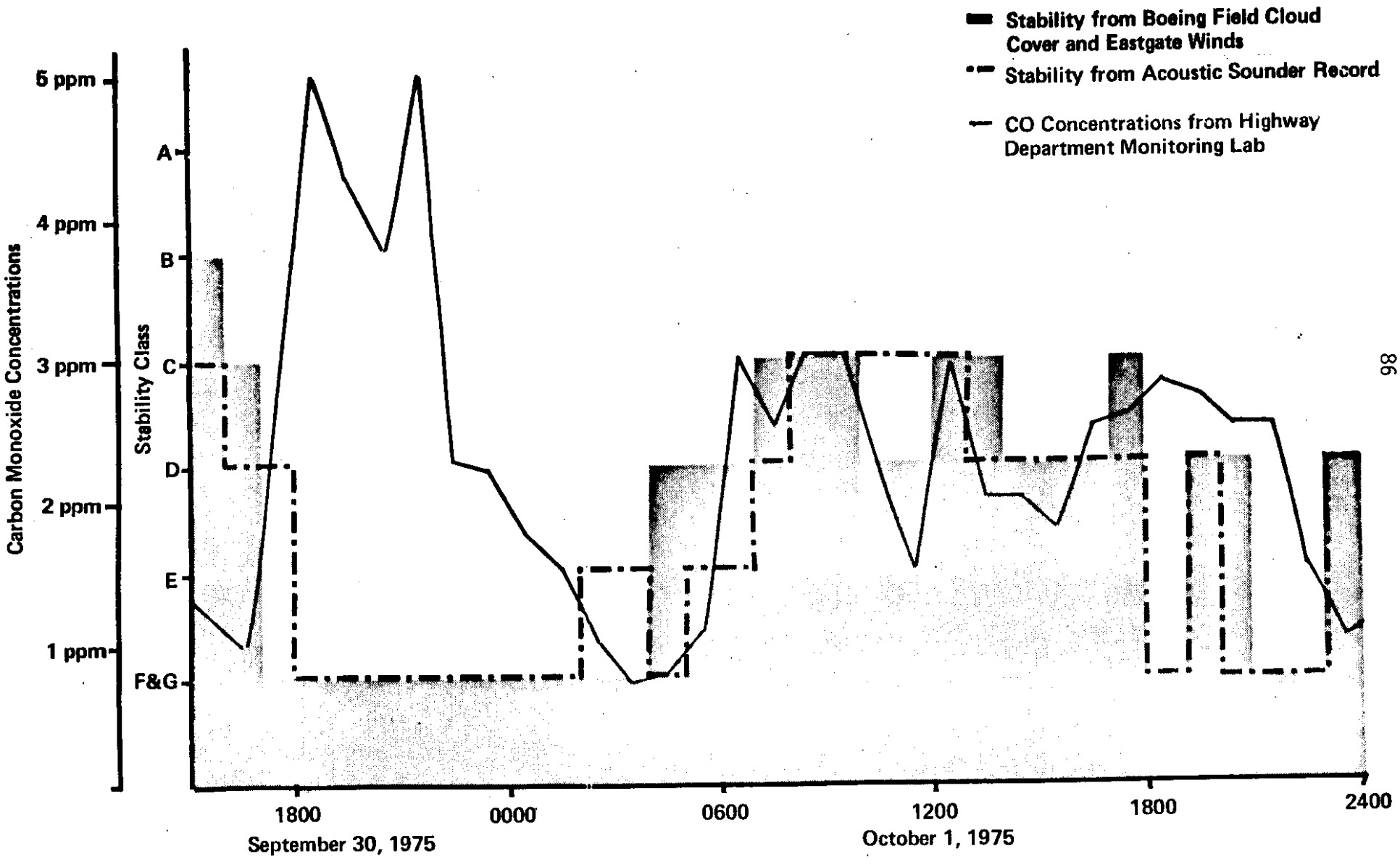

Figure 5. Comparison of Stability Classes Determined by Cloud Cover Data and from the Acoustic Sounder Record. Eastgate Site.

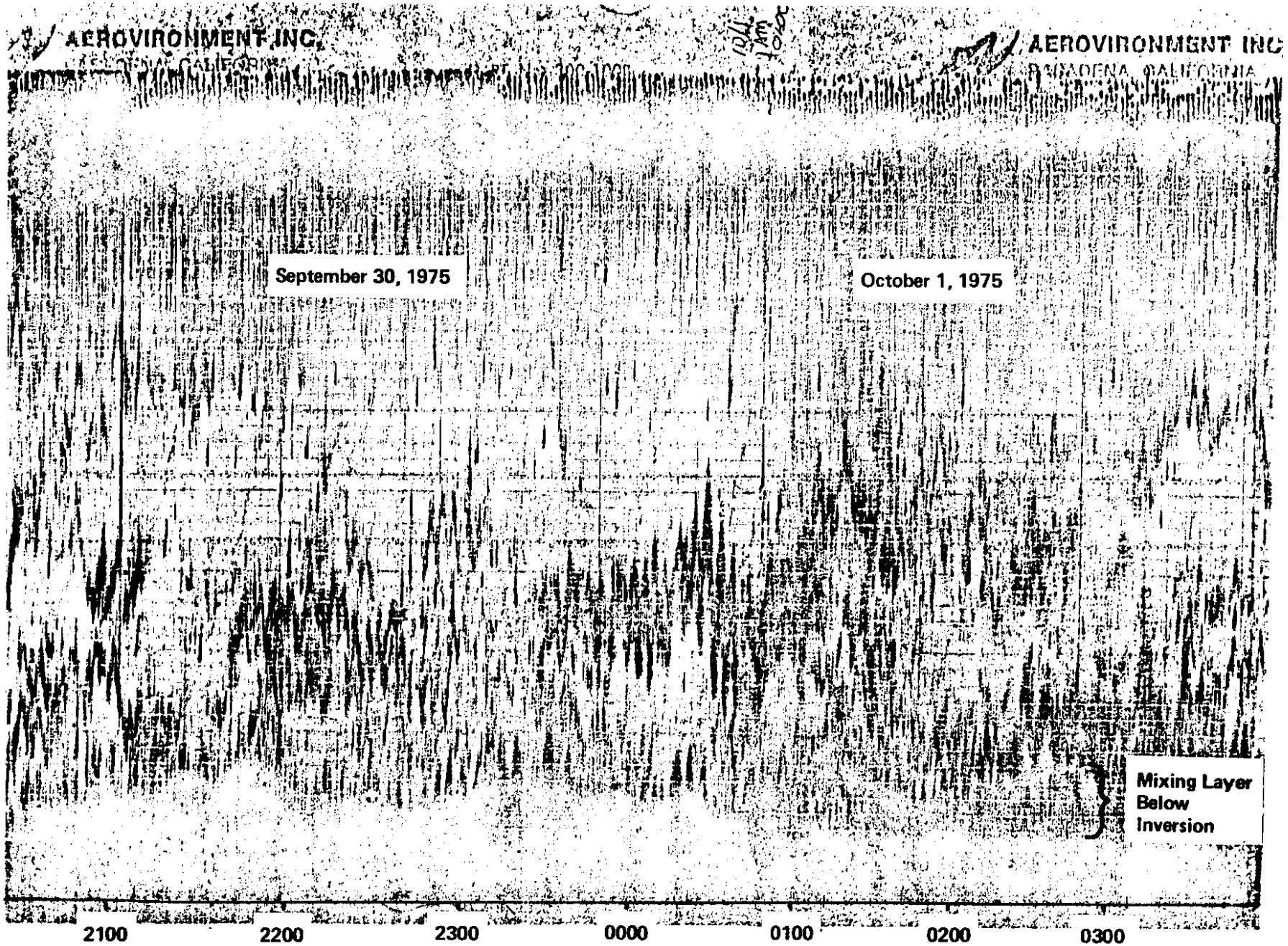

Figure 6. Acoustic Sounder Record for Part of the Period Shown in Figure 5. Note One Example of an Inversion with Evidence of Mixing Near the Surface. Eastgate Site.

to be segregated depending on whether the wind were blowing across the highway or from the trailer to the highway. There is not sufficient data in this set or from the Duwamish site to do this.

Because of the evidence of the periodic nature of the changes in stability and the duration of mixing layers near the ground, it is recommended that the proposed field study should consider taking air quality and meteorological data and traffic counts on a short enough time scale to allow the examination of improving model results by shortening the averaging time.

V. Conclusions

Examination of the above comparisons of various stability determinations shows that the acoustic radar derived mixed layer height is at least a reasonable indicator of stability class. In effect if a mean stability is formed from all available determinations, the radar derived stability follows it as well as any. The short periods of examination and the geographical peculiarities of each site make a more extensive comparison difficult and possibly outside the scope of this work. At present the situation with respect to stability class determination is complicated. Stability classes A and B characterizing strong convection are separated from all other classes by the existence of needle-like acoustic radar traces from the plumes. Stability classes C and D are identified by lack of trace or high inversion, E by low level inversion with mixing below, and F by low level inversion reach and group. At present a finer resolution is not available, but we feel it is possible using primarily if not solely the radar data.

A second conclusion is apparent. For stabilities higher than C the acoustic radar is measuring an inversion height. In this situation a box model or mixing height model is encouraged. These models have been discussed in earlier reports, but have not been emphasized. It now seems appropriate to reexamine one or more of these models with the exact heights from the acoustic radar as input.

Appendix B
Evaluation of Traffic Parameters

B1. Emission Sources

Mobile sources may be classified as line sources or area sources as follows:

In the line source method the study area is divided into parallel lines (traffic lanes in each direction of flow) and the lines are broken into short segments. Carbon monoxide emission rates for each segment are calculated from traffic flow density, using emission factors developed by EPA (10) and correcting them to reflect the traffic characteristics of the study area. The main traffic parameters are vehicle speed and traffic density. The EPA composite emission factors are functions of the vehicle speed. Various modes of traffic movements such as cruise, acceleration, deceleration and idle have to be evaluated and an averaged value has to be established for each line segment. The line source method is used in highway and street traffic emission studies.

B2. Traffic Parameters Used in the Study

In the EPA HIWAY air quality model used in this study CO concentration predictions were based on emission factors generated by the line source method. Main traffic parameters required to calculate emission factors were: traffic density, gate capacity, apparent vehicle speed in each segment and queuing characteristics of vehicles.

B2.1 Traffic Density

Traffic data were taken from the Freeway Surveillance Group of the Washington State Highway Department's District 1 office. Field traffic counts and toll booth records were also utilized in traffic studies. Peak traffic flow occurred during morning and evening rush hours. These periods

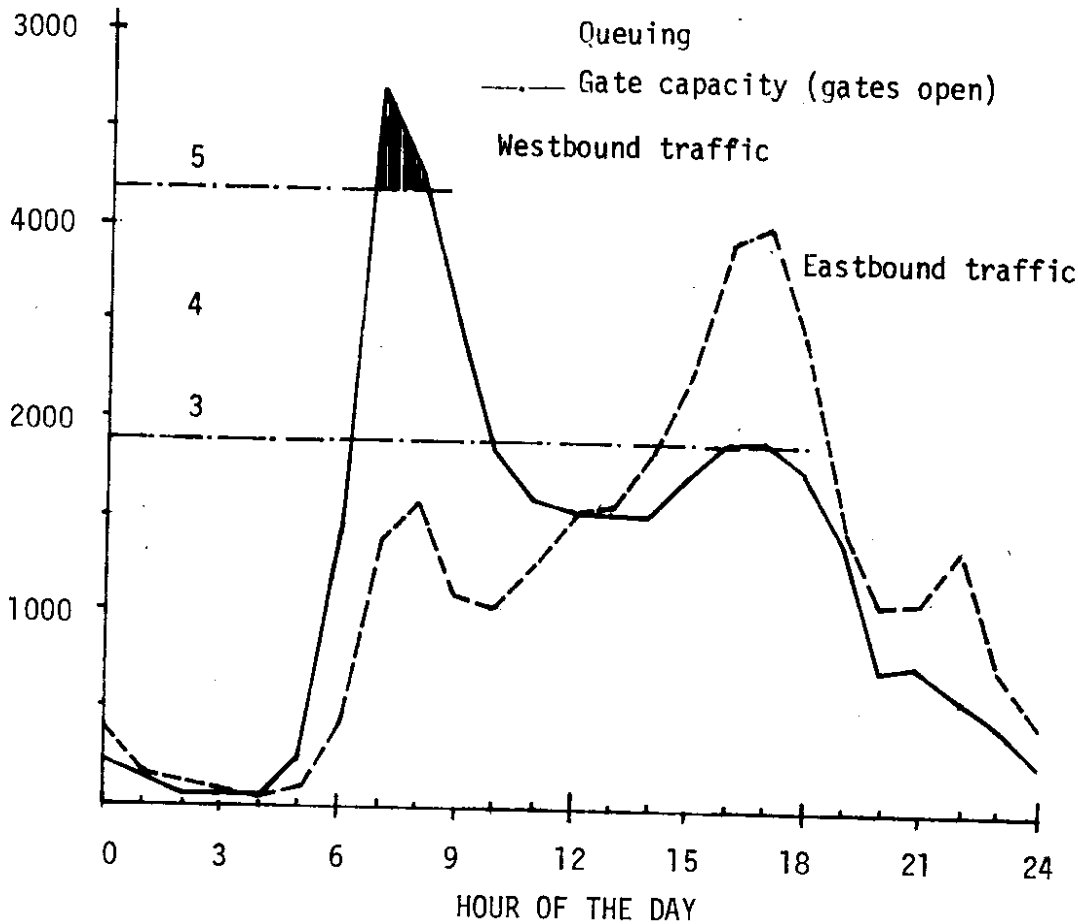

Figure B.1. Daily Traffic Profile (11.23.76)

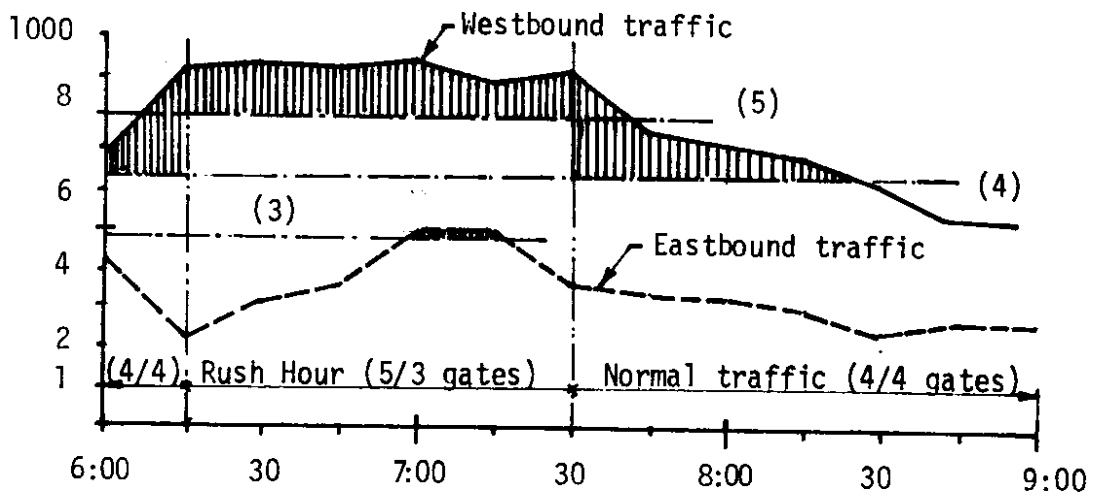

Figure B.2. Peak Hour Traffic Queuing (11.23.76)

were used as "worst emission" cases in this study. Figures B-1 and B-2 show a typical daily traffice profile and peak hour traffic variations respectively.

B2.2 Gate Capacity

There are eight gates with toll booths in the traffic area, one for each traffic lane, four lanes for each direction of traffic. For rush hour traffic five lanes were open in the heavy traffic and three in the opposite direction. Traffic flow characteristics through toll gates were observed and vehicle countings were made to establish the statistical average vehicle flow during rush hours. The time required for a vehicle to pass the toll booth varied from 3.5 sec/vehicle to 7 sec/vehicle and also varied from gate to gate. At toll booths used for vehicles with a pass the time was shorter. The gate time averaged from numerous continuous countings and for eight gates resulted in 5.5 sec/vehicle. Based on this time, the gate capacity (cars/period) was 160 cars/land in 15 minutes (traffic density data was only available for 15 minute accumulated periods). Table A.1 charts gate capacities for various traffic conditions.

Table B.1. Gate Capacity

Traffic	Gates Used	Vehicle Flow	
		in 15 minutes	in 1 hour
Rush hour, high traffic flow direction	5	800	3200
Normal Conditions	4	640	2560
Rush hour, low traffic direction	3	480	1920

B2.3 Apparent Vehicle Speed

The study area was divided into four source segments, S_1 through S_4, as shown in Figure 2. The second utility pole in each direction from the booths center-line was used as segment boundary. The distances were 186 feet and 200 feet respectively for west and east segments. Vehicle movement characteristics were evaluated for each segment. The unobstructed traffic moved at a speed limit of 50 mph (73.5 ft/sec) over the bridge and on the highway. Cars approaching the gates slowed down, stopped and accelerated after the gate to the 50 mph cruising speed. Car movements were observed and their residence times in the segments were measured. The statistical averages for the departure segments were 29 ft/sec and 31 ft/sec for S_1 and S_3 respectively. The traffic density did not affect this average speed. The apparent speeds in the approach segments S_2 and S_4 depended on the queuing characteristics of cars. A worst case, during rush hours, when the segments were occupied by line-up cars, the measured vehicle apparent speeds were 5.7 ft/sec (3.9 mph).

B2.4 Queuing

Queuing or piling up vehicles may occur when the steady state flow of vehicles is interrupted. This interruption may be for a preprogrammed period which is the case for the red/green traffic signal system or for an indefinite stopping period as is the case for stop signs and traffic booths. At stop signs the vehicle waiting time depends on the traffic flow in the crossing lane, when sufficiently long clearance is available between moving cars. At toll booths the stop period is more definite and depends on the time required to pay the toll (drop in coins, passes or wait for change). A statistical average waiting period of 5.5 seconds was established for a vehicle passing the toll booth(see paragraph B2.2). The front bumper to front bumper distance, assuming an average car length of 20 feet (11), was

24 feet when solid care pile up developed. Observations indicated that, because of the frequent stop-start of vehicles during queuing (initiated by the vehicles stop/start at the booths) the vehicles kept an average of 36 feet distances. Based on this figure an average speed of 5.7 feet/second was established for vehicles in a developed queuing line. The apparent speed in an approach segment (S_2, S_4) depended on the number of queuing vehicles and was calculated as 18 feet/second for free flow(no queuing) and 5.7 feet/second for fully developed queuing in the source segment (7 or more queuing cars). Because of the temporal distribution of vehicles (vehicles do not arrive at the gate in equal time intervals) queuing can occur even during light traffic conditions. Observation indicated that an average of 2-3 vehicles were queuing in the approaching segments even during medium heavy traffic conditions and the corresponding apparent speed was calculated at 9 feet/second.

Theoretically, queuing will start to develop when the traffic density exceeds the gate capacity. This case is shown in Figure B.1 for 15 minutes and one hour accumulated vehicle density. Traffic data indicated that the traffic density exceeded quite frequently the gate capacity and queuing of vehicles occurred during rush hours. For this reason the use of the queuing speed of 5.7 feet/second (3.9 mph) was suggested for emission factor calculations.

There are several other factors which could affect the development of queuing such as forced slow down of vehicles, changes in number of lanes, changes of distances between cars, etc. These factors were not explored in this study.

B.3. Computer input

The results of the traffic study are charted in Table A.2 below.

Table B.2. Apparent Speeds

Segment	Calculated from empirical data		Used for Emission Factor Calculation[b] mph
S_1 S_3	21.0	30.0[a]	20
S_2 S_4	3.9	5.7	5

Notes: (a) Average value of 29 ft/sec and 31 ft/sec
(b) Rounded to nearest 5 mph bracket

Appendix C

Infrared Analysis Specifications

SPECIFICATIONS

OPERATING RANGES
Instrument supplied, as ordered, with either one range or three ranges. Range 1 is provided with the sensitivity required for the particular application; refer to Factory Data Sheet supplied with the instrument. Optional Ranges 2 and 3 have adjustable sensitivity. With standard multiple-range configuration, fullscale meter reading on Range 2 corresponds to reading of between 71% and 26% on Range 1, fullscale reading on Range 3 corresponds to reading of between 62% and 18% on Range 1. In an alternative configuration, fullscale reading on Range 2 corresponds to reading of between 100% and 38% on Range 1; fullscale reading on Range 3 corresponds to reading of between 91% and 25% on Range 1. Refer to Paragraphs 4.1.4 and 4.1.5.

*MAXIMUM ZERO DRIFT**
±1% of fullscale per 24 hours.

*MAXIMUM SPAN DRIFT**
±1% of fullscale per 24 hours.

SENSITIVITY
0.5% of fullscale.

ACCURACY
±1%.

AMPLIFIER RESPONSE SPEED
90% response in 0.5 second is standard.

NOISE LEVEL
1% of fullscale, as measured on recorder with response time of less than 1 second.

AMBIENT TEMPERATURE RANGE
Model 215B: +60°F to +105°F.
Models 315B(S) and 415B(S): +30°F to +120°F.
Models 315B(L) and 415B(L): +50°F to +120°F.

OUTPUTS
Potentiometric-output instrument:
0 to 10 mv
0 to 100 mv
0 to 1 volt
0 to 5 volts.

Current-output instrument:

Outputs (ma)	Maximum Permissible Load (ohms)
0 to 5	800
1 to 5	8000
4 to 20	2000
10 to 50	700

VOLTAGE AND FREQUENCY
Instrument operates on either:
115 ±15 volts, 60 ±0.5 Hz; or
115 ±15 volts, 50 ±0.5 Hz.

MAXIMUM POWER CONSUMPTION
Model 215B: 160 watts.
Model 315B(S): 300 watts.
Model 315B(L): 410 watts.
Model 415B(S): 300 watts.
Model 415B(L): 410 watts.

MAXIMUM SEPARATION OF AMPLIFIER/CONTROL SECTION AND ANALYZER SECTION
1000 feet.

SHIPPING WEIGHT
Model 215B: 75 pounds.
Model 315B(S): 115 pounds.
Model 315B(L): 170 pounds.
Model 415B(S): 145 pounds.
Model 415B(L): 156 pounds.

NET WEIGHT
Model 215B: 65 pounds.
Model 315B(S): 85 pounds.
Model 315B(L): 120 pounds.
Model 415B(S): 110 pounds.
Model 415B(L): 106 pounds.

CATALOG NUMBERS
190100 Model 215B Infrared Analyzer.
190101 Model 315B(S) Infrared Analyzer (Short Path).
190102 Model 315B(L) Infrared Analyzer (Long Path).
190103 Model 415B(S) Infrared Analyzer (Short Path).
190104 Model 415B(L) Infrared Analyzer (Long Path).

**Span and zero drift specifications are based on ambient temperature shifts of less than 20°F at a maximum rate of 20°F per hour.*

Appendix D

Acoustic Radar Modifications

The Acoustic Radar used in this study was a Model 300C Monostatic System manufactured by Aerovironment Inc., Pasadena, California, modified according to specifications provided by the University of Washington. A description of the basic commercial model is contained on the following page. The antenna was fabricated at the University in order to optimize the design for the situation in which the system was to operate. Several manufacturer's options and modifications were exercised in the Acoustic Radar purchase:

1) Extra power delivered to the transducer during transmit
2) A carrier frequency of 2750 Hz, well above the 1600 Hz standard for the manufacturer
3) A short (20 msec) transmit pulse among the three selectrable pulse lengths.
4) High speed stylus motion producing full scale ranges of about 300 and 600 meters.

These options were chosen to resolve the boundary layer of this geographical region with the requisite detail under circumstances of very high traffic noise. The primary design requirement behind the antenna construction was also environmental noise. The University of Washington antenna is taller and more opaque to sound than the antenna available from the manufacturer. Also, the UW antenna is tapered while the manufacturer design has parallel sides. Each of these variations on the manufactuer design contributes significantly to environmental noise suppression. Finally, the University of Washington antenna can be knocked down and moved with expenditure of reasonable effort.

SPECIFICATIONS

SPECIFICATIONS OF MODEL 300 ACOUSTIC RADAR

Transmitted Pulse:	Frequency – 1600 Hz Duration – selectable 50, 100, or 200 ms Power Input – 25 W Repetition Rate – 1 per 9 seconds (500 m scale) – 1 per 18 seconds (1 km scale)
Receiver:	Gain – 10^8 Gain Compensation – proportional to time of echo return, with additional adjustment possible for short ranges Bandwidth – less than 20, 40 and 80 Hz (between –3 dB points, 72 dB/octave cutoff) switch selectable Range – Selectable 1 km or 500 m full scale – Minimum 20 m Resolution – 20 m
Recorder:	Writing Technique – electric on conducting chart paper Chart size – 6" (15.2 cm) wide by 72' (22 m) Chart speed – 1.2" (3.05 cm) per hour Chart duration – 28 days
Sound Level (with Model 301 Acoustic Enclosure)	Transmitted horizontally – < 60 dBA at 10 m Maximum Desirable Ambient – approximately 68 dbA for 1 km scale, 74 dBA for 500 m scale
Size and Weight:	Electronics and Recorder – 17" W x 17" H x 6" D, 45 lbs (43 cm W x 43 cm H x 15 cm D, 18 kg) Antenna and Transducer – 52" dia x 36" H, 58 lbs (133 cm dia x 80 cm H, 23 kg)
Power Input:	115 V, 60 Hz, 50 W average, 250 W peak during pulse transmission

AEROVIRONMENT INC.
145 VISTA AVE. PASADENA, CA 91107 • 213-4494392

Appendix E

Pasquill-Turner Stability Classes

JOB NO. 13530 SEASONAL & ANNUAL

WIND DISTRIBUTION BY PASQUILL STABILITY CLASSES (STAR PROGRAM) (5 Classes) (8 Obs/Day)

STATION: #24229, Portland, Oregon/WBAS PERIOD: Jan. 1967 - Dec. 1971

Data are presented by stability classes and also combined for the period indicated; first, as a bivariate frequency distribution of wind direction vs. wind speed, and second, as normalized values (i.e., relative frequency). Stability classes used are based on Pasquill's class structure (see Journal of Applied Meteorology, February 1964), as follows:

Pasquill Stability Class	Identified in lower left corner in this tabulation as		Definition
1	A		Extremely Unstable
2	B		Unstable
3	C		Slightly Unstable
4	D		Neutral
5	E	E	Slightly Stable
6-7	F		Stable to Extremely Stable

Average wind speed in knots, to tenths, for each direction and each speed class. Overall average wind speed is computed by

$$\frac{\text{Sum of wind speed}}{\text{Number of occurrences}}$$

NUMBER OF OCCURRENCES: Number of DIR/SPD observations, plus number of calms (winds are tabulated to 16 points; speeds are in knots.)

RELATIVE FREQUENCY OF OCCURRENCES: $\frac{\text{Number of occurrences/stability class}}{\text{Total number of observations}}$

TOTAL NUMBER OF OBSERVATIONS: Number of observations in each, month, season, annual or period.

TOTAL RELATIVE FREQUENCY OF OBSERVATIONS: $\frac{\text{Total number of observations}}{\text{Total number of observations}} = 1.00000$

This normalized (relative frequency) table is self explanatory, except that the calm values have been distributed in the 0-3 speed category based on the number of observations in speed categories 0-3 and 4-6.

Example: Total Obs (N) = 3601 (DJF) $\quad \frac{\text{Number of calms in "C" class (2)}}{\text{N (3601)}} = .0005554 \quad \frac{.0005554}{(30)\ \text{Number obs. in classes 1-3 and 4-6}} = .0000185$

From the South direction there are seven observations in the first two speed categories, hence 7(.0000185) = .0001295
In the first category there are 2 observations. 2/3601=.0005554 When added together .0005554 + .0001295=.0006849 the resultant (.000685) figure is placed in the South 0-3 category and .00389 in the South 4-6 category. This method is used to distribute the calms into the 0-3 speed category, by directions.

Appendix E continued

The following explanation of the Pasquill Stability classification has been extracted from an article by D. Bruce Turner in the February 1964 Journal of Applied Meteorology.

This system of classifying stability on an hourly basis for research in air pollution is based upon work accomplished by Dr. F. Pasquill of the British Meteorological Office (1961). Stability near the ground is dependent primarily upon net radiation and wind speed. Without the influence of clouds, insolation (incoming radiation) during the day is dependent upon solar altitude, which is a function of time of day and time of year. When clouds exist their cover and thickness decrease incoming and outgoing radiation. In this system insolation is estimated by solar altitude and modified for existing conditions of total cloud cover and cloud ceiling height. At night estimates of outgoing radiation are made by considering cloud cover. This stability classification system has been made completely objective so that an electronic computer can be used to compute stability classes. The stability classes are as follows: 1) Extremely unstable, 2) Unstable, 3) Slightly unstable, 4) Neutral, 5) Slightly stable, 6) Stable, 7) Extremely stable. Table A-1 gives the stability class as a function of wind speed and net radiation. The net radiation index ranges from 4, highest positive net radiation (directed toward the ground), to -2, highest negative net radiation (directed away from the earth). Instability occurs with high positive net radiation and low wind speed, stability with high negative net radiation and light winds, and neutral conditions with cloudy skies or high wind speeds.

The net radiation index used with wind speed to obtain stability class is determined by the following procedure:

1) If the total cloud cover is 10/10 and the ceiling is less than 7000 feet, use net radiation index equal to 0 (whether day or night).

2) For night-time (night is defined as the period from one hour before sunset to one hour after sunrise):
   a) If total cloud cover $\leq$ 4/10, use net radiation index equal to -2.
   b) If total cloud cover $>$ 4/10, use net radiation index equal to -1.

3) For daytime:
   a) Determine the insolation class number as a function of solar altitude from Table A-2.
   b) If total cloud cover $\leq$ 5/10, use the net radiation index in Table A-1 corresponding to the insolation class number.
   c) If cloud cover $>$ 5/10, modify the insolation class number by following these six steps:
      1) Ceiling $<$ 7000 ft, subtract 2.
      2) Ceiling $\geq$ 7000 ft but $<$ 16,000 ft, subtract 1.
      3) Total cloud cover equal 10/10, subtract 1. (This will only apply to ceilings $\geq$ 7000 ft since cases with 10/10 coverage below 7000 ft are considered in item 1 above.)
      4) If insolation class number has not been modified by steps (1), (2), or (3) above, assume modified class number equal to insolation class number.
      5) If modified insolation class number is less than 1, let it equal 1.
      6) Use the net radiation index in Table A-1 corresponding to the modified insolation class number.

Since urban areas do not become as stable in the lower layers as non-urban areas, stability classes 5, 6 and 7 computed using the STAR program may be combined into a single class (5), or classes 6 and 7 may be combined and identified as class 6.

Appendix E continued

TABLE A-1. STABILITY CLASS AS A FUNCTION OF NET RADIATION AND WIND SPEED

WIND SPEED (KNOTS)	NET RADIATION INDEX						
	4	3	2	1	0	-1	-2
0, 1	1	1	2	3	4	6	7
2, 3	1	2	2	3	4	6	7
4, 5	1	2	3	4	4	5	6
6	2	2	3	4	4	5	6
7	2	2	3	4	4	4	5
8, 9	2	3	3	4	4	4	5
10	3	3	4	4	4	4	5
11	3	3	4	4	4	4	4
≥12	3	4	4	4	4	4	4

TABLE A-2. INSOLATION AS A FUNCTION OF SOLAR ALTITUDE

SOLAR ALTITUDE (α)	INSOLATION	INSOLATION CLASS NUMBER
$60° < \alpha$	Strong	4
$35° < \alpha \leq 60°$	Moderate	3
$15° < \alpha \leq 35°$	Slight	2
$\alpha \leq 15°$	Weak	1

Appendix F

Computer Model Predictions

Toll Plaza 11/23/76 Stability = 4

Wind = 180°

Line Source	Receptor 1	2	3	4	5	6
1	1.148	.000	.000	.020	.000	*
2	.000	.000	.000	.002	.000	*
3	.000	.000	.000	14.914	15.673	9.984
4	*	.000	.000	1.619	1.758	1.083
Total	1.148	.000	.000	16.533	17.431	11.067

15.0

Wind = 210°

Line Source	Receptor 1	2	3	4	5	6
1	.528	.154	.000	4.522	1.278	.000
2	.000	*	*	1.284	.067	.000
3	.000	.000	.000	9.404	17.264	16.922
4	.000	.000	.043	.270	1.294	2.001
Total	.528	.154	.043	15.480	19.903	18.923

18.1

Wind = 225°

Line Source	Receptor 1	2	3	4	5	6
1	.321	.479	.000	7.155	5.624	.043
2	.000	*	*	3.896	.950	.000
3	.000	.000	.000	3.460	16.354	21.174
4	.000	.000	.132	.012	.383	2.299
Total	.321	.479	.132	14.523	23.311	23.516

20.5

Toll Plaza 11/23/76 Stability = 5

Wind = 180°

Line Source	Receptor 1	2	3	4	5	6
1	1.144	.000	.000	.006	.000	*
2	.000	.000	.000	.001	.000	*
3	.000	.000	.000	15.535	15.890	10.183
4	*	.000	.000	1.780	1.871	1.164
Total	1.144	.000	.000	17.322	17.761	11.348

15.5

Wind = 210°

Line Source	Receptor 1	2	3	4	5	6
1	.533	.143	.000	5.182	1.170	.000
2	.000	*	*	1.265	.037	.000
3	.000	.000	.000	9.916	17.816	17.251
4	.000	.000	.040	.236	1.429	2.142
Total	.533	.143	.040	16.599	20.452	19.393

18.8

Wind = 225°

Line Source	Receptor 1	2	3	4	5	6
1	.324	.448	.000	8.178	6.388	.013
2	.000	*	*	4.299	.872	.000
3	.000	.000	.000	3.258	17.182	21.668
4	.000	.000	.123	.005	.355	2.521
Total	.324	.448	.123	15.740	24.797	24.202

21.6

Toll Plaza 10/29/76 Stability = 4

Wind = 180°

Line Source	Receptor 1	2	3	4	5	6
1	2.449	.000	.000	.043	.000	*
2	.000	.000	.000	.004	.000	*
3	.000	.000	.000	26.302	27.641	17.607
4	*	.000	.000	3.384	3.677	2.263
Total	2.449	.000	.000	29.733	31.318	19.870

27.0
(18.0, 50%)

Wind = 210°

Line Source	Receptor 1	2	3	4	5	6
1	1.127	.327	.000	9.647	2.727	.000
2	.000	*	*	2.219	.115	.000
3	.000	.000	.000	16.586	30.446	29.843
4	.000	.000	.090	.565	2.705	4.185
Total	1.127	.327	.090	29.017	35.993	34.028

33.0
(22.1, 49%)

Wind = 225°

Line Source	Receptor 1	2	3	4	5	6
1	.685	1.022	.000	15.263	11.996	.092
2	.000	*	*	6.733	1.642	.000
3	.000	.000	.000	6.102	28.842	37.342
4	.000	.000	.275	.024	.800	4.807
Total	.685	1.022	.275	28.122	43.280	42.241

37.9
(25.4, 49%)

Toll Plaza 10/29/76 Stability = 4

Zero Cold Start Vehicles

Wind = 180°

Line Source	Receptor 1	2	3	4	5	6
1	1.635	.000	.000	.029	.000	*
2	.000	.000	.000	.003	.000	*
3	.000	.000	.000	17.558	18.452	11.754
4	*	.000	.000	2.305	2.504	1.542
Total	1.635	.000	.000	19.895	20.956	13.296

18.0

Wind = 210°

Line Source	Receptor 1	2	3	4	5	6
1	.752	.219	.000	6.440	1.821	.000
2	.000	*	*	1.511	.078	.000
3	.000	.000	.000	11.072	20.325	19.922
4	.000	.000	.061	.385	1.843	2.851
Total	.752	.219	.061	19.408	24.067	22.773

22.1

Wind = 225°

Line Source	Receptor 1	2	3	4	5	6
1	.457	.682	.000	10.189	8.008	.062
2	.000	*	*	4.586	1.118	.000
3	.000	.000	.000	4.074	19.254	24.928
4	.000	.000	.188	.016	.545	3.274
Total	.457	.682	.188	18.865	28.925	28.264

25.4

Toll Plaza 10/29/76 Stability = 5

Wind = 180°

Line Source	Receptor 1	2	3	4	5	6
1	1.629	.000	.000	.009	.000	*
2	.000	.000	.000	.001	.000	*
3	.000	.000	.000	18.290	18.707	11.989
4	*	.000	.000	2.535	2.665	1.660
Total	1.629	.000	.000	20.835	21.372	13.649

18.6

Wind = 210°

Line Source	Receptor 1	2	3	4	5	6
1	.759	.204	.000	7.380	1.666	.000
2	.000	*	*	1.490	.044	.000
3	.000	.000	.000	11.674	20.975	20.310
4	.000	.000	.057	.336	2.036	3.051
Total	.759	.204	.057	20.880	24.721	23.361

23.0

Wind = 225°

Line Source	Receptor 1	2	3	4	5	6
1	.462	.638	.000	11.646	9.097	.019
2	.000	*	*	5.061	1.027	.000
3	.000	.000	.000	3.835	20.228	25.510
4	.000	.000	.175	.007	.506	3.590
Total	.462	.638	.175	20.549	30.858	29.119

26.8

EPA HIWAY 11/3/76 Stability = 4

Wind = 180°

Line Source	Receptor 1	2	3	4	5	6
1	1.488	.000	.000	.026	.000	*
2	.000	.000	.000	.003	.000	*
3	.000	.000	.000	17.347	18.230	11.612
4	*	.000	.000	2.098	2.279	1.403
Total	1.488	.000	.000	19.474	20.509	13.015

17.666

Wind = 210°

Line Source	Receptor 1	2	3	4	5	6
1	.685	.199	.000	5.861	1.657	.000
2	.000	*	*	1.493	.077	.000
3	.000	.000	.000	10.939	20.080	19.683
4	.000	.000	.056	.351	1.677	2.594
Total	.685	.199	.056	18.644	23.491	22.277

21.471

Wind = 225°

Line Source	Receptor 1	2	3	4	5	6
1	.416	.621	.000	9.273	7.288	.056
2	.000	*	*	4.532	1.105	.000
3	.000	.000	.000	4.025	19.022	24.628
4	.000	.000	.171	.015	.496	2.980
Total	.416	.621	.171	17.845	27.911	27.664

24.473

EPA HIWAY 11/3/76 Stability = 5

Wind = 180°

Line Source	Receptor 1	2	3	4	5	6
1	1.482	.000	.000	.008	.000	*
2	.000	.000	.000	.001	.000	*
3	.000	.000	.000	18.070	18.482	11.845
4	*	.000	.000	2.307	2.426	1.510
Total	1.482	.000	.000	20.386	20.908	13.355

18.216

Wind = 210°

Line Source	Receptor 1	2	3	4	5	6
1	.691	.186	.000	6.716	1.516	.000
2	.000	*	*	1.472	.043	.000
3	.000	.000	.000	11.533	20.723	20.065
4	.000	.000	.052	.306	1.853	2.777
Total	.691	.186	.052	20.027	24.135	22.842

22.335

Toll Plaza 11/3/76 Stability = 6

Wind = 180°

Line Source	Receptor 1	2	3	4	5	6
1	1.475	.000	.000	.001	.000	*
2	.000	.000	.000	.000	.000	*
3	.000	.000	.000	18.538	18.529	11.956
4	*	.000	.000	2.501	2.548	1.607
Total	1.475	.000	.000	21.040	21.077	13.563

18.560

Wind = 210°

Line Source	Receptor 1	2	3	4	5	6
1	.691	.182	.000	7.676	1.322	.000
2	.000	*	*	1.420	.020	*
3	.000	.000	.000	11.978	21.081	20.188
4	.000	.000	.051	.248	2.027	2.933
Total	.691	.182	.051	21.322	24.450	23.121

23.0

Wind = 225°

Line Source	Receptor 1	2	3	4	5	6
1	.420	.558	.000	12.044	9.348	.002
2	.000	*	*	5.449	.909	.000
3	.000	.000	.000	3.501	20.714	25.455
4	.000	.000	.153	.002	.411	3.537
Total	.420	.558	.153	20.996	31.382	28.994

27.1

Appendix G

Mixing Height vs CO Concentration

Date,	Time	(Zi) Mixing Height*	Carbon Monoxide (ppm)*
10/8/76	(0750)	50	20
	(1600)	50	21
10/29	(0750)	60	19
	(1600)	70	13
11/1	(0750)	70	16
	(1600)	60	15
11/2	(0750)	50	17
	(1600)	60	15
11/3	(0750)	50	19
	(1600)	50**	17
11/4	(0750)	70	17
	(1600)	30**	22
11/10	(0750)	60	12
	(1600)	no trace	-
11/12	(0750)	75	13
	(1600)	85	11
11/15	(0750)	85	10
	(1600)	60	13
11/18	(0750)	90	12
	(1600)	no trace	-
11/19	(0750)	90	13
	(1600)	60	13
11/22	(0750)	60	13
	(1600)	55	13
11/23	(0750)	80	10
	(1600)	no trace	-

* Averaged over 1 hour period
** light trace

r = -.77
m = .18
b = 26.8

Average maximum mixing height compared to average CO concentration

Appendix H
Stability Comparison Data
Pasquill-Turner Method (P-T)
Acoustic Radar Method (A-R)

DATE	TIME	CLOUD	WIND (MPH)	NRI	STABILITY	(P-T)	(A-R)
11/1	0730	SCT	3	-2	7 =	F	F
	1645	OVC	1	0	4 =	D	E
11/2	0730	OVC	2	0	4 =	D	E
	1515	OVC	2	0	4 =	D	E
11/3	0730	CLR	2	-2	7 =	F	F
	1530	CLR	2	-2	7 =	F	E
11/4	0730	FOG	2	-1	6 =	E	E
	1530	CLR	2	-2	7 =	F	E
11/5	0730	FOG	2	-1	6 =	E	E
	1345	OVC	2	1	3 =	C	C
11/6	-	OVC					
	-						
11/7	-						
	1600	OVC	2	0	4 =	D	D
11/8	0730	OVC		0	4 =	D	E
	1600	OVC		0	4 =	D	E
11/9	0730	OVC	3	0	4 =	D	D
	1545	OVC	2	0	4 =	D	C
11/10	0730	FOG	1	0	4 =	D	D
	1545	HAZE	1	0	4 =	D	E
11/11	0730	FOG	1	0	4 =	D	E
	1600	CLR	2	-2	7 =	D	E
11/12	0730	FOG	1	0	4 =	D	E
	-						
11/13	-						
11/14	-						
11/15	0730	OVC	4	0	4 =	D	F
	1615	OVC	2	0	4 =	D	F
11/16	-						
11/17	-	OVC	10				
11/18	0730		1	0	4 =	D	F
	1500	OVC	2	0	4 =	D	D
11/19	1000	OVC	2	0	4 =	D	D
	1500	OVC	3	0	4 =	D	D
11/20	1000	SCT		1	3 =	C	E
	-						
11/21	-						
	1530	OVC	2	0	4 =	D	D

DATE	TIME	CLOUD	WIND (MPH)	NRI	STABILITY (P-T)	(A-R)
11/22	0730	OVC	2	0	4 = D	E
	1515	OVC	2	0	4 = D	D
11/23	0730	OVC	2	0	4 = D	E
	1600	OVC	3	0	4 = D	D
11/24	0730	OVC	10	0	D	D
	1600	OVC	8	0	D	D
11/25	0900	OVC				
11/26	0930	CLR	2			
11/29	0730	SCT	2	-2	F	F
	1500	SCT	2	-2	F	F
11/30	0730	FOG	-	0	D	E
	1515	CLR	2	-2	F	F
12/1	0730	FOG	2	0	D	E
	1500	FOG	2	0	D	E
12/2	0730	FOG	2	0	D	E
	1500	FOG	2	0	D	E
12/3	0730	FOG	-	0	D	D
	1520	OVC	2	0	D	D
12/6	0730	OVC	2	0	D	D
	1600	OVC	7	0	D	D
12/7	0730	OVC	10 - 15	0	D	D
	-	SCT	-	-2	D	D
12/8	0730	SCT	-	-2		
	1600					
12/10	?	OVC	7			
12/11	1000	OVC	5	0	D	D
12/12	1000	FOG	3	0	D	E
	1600	SCT	5	-2	F	F
12/13	0730	OVC	6	0	D	D
	1530	SCT	3	-2	F	F
12/14	0730	OVC	6	0	D	E
	1530	SCT	5	-2	F	F
12/15	0730	OVC	8	0	D	E
	1515	SCT	15	-2	D	D